FOXO1 represses *Sprouty2* and *Sprouty4* expression to promote arterial specification and vascular remodeling in the mouse yolk sac

Nanbing Li-Villarreal*, Rebecca Lee Yean Wong*, Monica D. Garcia*, Ryan S. Udan, Ross A. Poché, Tara L. Rasmussen, Alexander M. Rhyner, Joshua D. Wythe, and Mary E. Dickinson**

Department of Molecular Physiology & Biophysics, Baylor College of Medicine. One Baylor Plaza, Houston, Texas 77030.

* Authors who contributed equally to the work

** Correspondence: mdickins@bcm.edu

ABSTRACT

Establishing a functional circulatory system is required for post-implantation development during murine embryogenesis. Previous studies in loss-of-function mouse models showed that FOXO1, a Forkhead family transcription factor, is required for yolk sac (YS) vascular remodeling and survival beyond embryonic day (E) 11. Here, we demonstrate that at E8.25, loss of *FoxO1* in *Tie2-cre* expressing cells resulted in increased *Sprouty2* and *Sprouty4,* reduced arterial genes, and reduced *Flk1/Vegfr2* transcripts without affecting overall endothelial cell identity, survival, or proliferation. Using a *Dll4-BAC-nlacZ* reporter line, we found that one of the earliest expressed arterial genes, *Delta like 4*, is significantly reduced in *FoxO1* mutant YS without being substantially affected in the embryo proper. We show that FOXO1 binds directly to previously identified *Sprouty2* gene regulatory elements (GREs) and newly identified, evolutionarily conserved *Sprouty4* GREs to repress their expression. Furthermore, overexpression of *Sprouty4* in transient transgenic embryos largely recapitulates reduced arterial genes seen in

conditional *FoxO1* mutants. Together, these data reveal a novel role for FOXO1 as a key transcriptional repressor regulating both pre-flow arterial specification and subsequent vessel remodeling within the murine YS.

INTRODUCTION

During early development the mammalian embryo requires a functional circulatory system to distribute oxygen, nutrients, and hormones. The mammalian heart is the first organ to form and function within this early embryo, along with the first arteries and veins that arise de novo via vasculogenesis (Fish and Wythe, 2015, Risau, 1994, Risau and Flamme, 1995, Chong et al., 2011). Primitive erythrocytes form in the blood islands of the extra-embryonic yolk sac (YS), and are drawn into circulation as the heart begins to beat around embryonic day (E) 8 in the mouse embryo (Lucitti et al., 2007, Palis, 2014, Ji et al., 2003). A complete circulatory loop between the embryo and the extra-embryonic YS is evident shortly after the onset of cardiac contractions, with blood flowing through the dorsal aorta to the vitelline (omphalomesenteric) artery (VA), through the YS capillary plexus, and back through the vitelline (omphalomesenteric) vein (VV) to the sinus venosus of the heart. Circulation through the YS is the main circulatory loop until the chorio-allantoic placenta connections develop later around E9.

A key finding several years ago showed that arterial-venous (AV) identity is established prior to the onset of blood flow in the early mouse embryo (Herzog et al., 2005, Chong et al., 2011, Aitsebaomo et al., 2008, Wang et al., 1998, Adams et al., 1999). Others have since shown that some aspects of AV identity are plastic, as they can be influenced by changes in blood flow and hemodynamics (le Noble et al., 2004, le Noble et al., 2005, Wragg et al., 2014). Extensive work in zebrafish showed that AV specification depends on differential responses to VEGF signaling through the tyrosine kinase receptor VEGFR2/Flk1, high levels of which activate the MEK/ERK kinase cascade in arterial cells and PI3K/AKT signaling in venous cells (Fish and Wythe, 2015, Covassin et al., 2006, Weinstein and Lawson, 2002). In the arterial

endothelium, VEGFR2 signaling stimulates the Notch pathway, which in turn promotes an arterial identity while simultaneously repressing a venous fate (Weinstein and Lawson, 2002, Krebs et al., 2010, Lawson et al., 2001, Lawson et al., 2002, Liu et al., 2003, Shutter et al., 2000, Swift and Weinstein, 2009, Siekmann and Lawson, 2007, Krebs et al., 2000, Duarte et al., 2004, Lobov et al., 2007). VEGF upregulates expression of *Delta-like 4 (Dll4),* which encodes a ligand for the Notch family of transmembrane receptors. *Dll4* is the earliest Notch ligand expressed in arterial cells in the early mouse embryo (Shutter et al., 2000, Mailhos et al., 2001, Wythe et al., 2013, Cleaver and Krieg, 1998, Chong et al., 2011), and is essential for AV patterning (Krebs et al., 2000, Gale et al., 2004, Duarte et al., 2004). Expression of *Dll4* depends on the activation of ETS transcription factors, downstream of VEGF signaling (Wythe et al., 2013, Fish et al., 2017) and *Dll4* mRNA expression can be increased by shear stress (Masumura et al., 2009, Obi et al., 2009). However, the expression of *Dll4* and a few other select arterial markers prior to, and independent of, the onset of blood flow (Chong et al., 2011, Wang et al., 1998) suggests flow-independent mechanisms regulate arterial specification. Vegfr2 also upregulates expression of the main endothelial cell surface receptor for Dll4, Notch1 (Lawson et al., 2002). Notch itself is activated by blood flow and the strength of this signal depends on the magnitude of shear stress (Masumura et al., 2009, Mack et al., 2017). Notch regulates cell junctions, cell cycle arrest, and induces an arterial gene expression program via a connexin37 (*Gja4*)/$p27^{Kip1}$ (*Cdkn1B*) pathway (Mack et al., 2017, Su et al., 2018, Fang et al., 2017). Critically, both Vegfr2 and Notch1 are thought to act as mechanosensors, likely linking arterial specification of ECs and hemodynamic feedback via blood flow to re-enforce and solidify their arterial identity (Mack et al., 2017, Tzima et al., 2005, Mack and Iruela-Arispe, 2018, Shay-Salit et al., 2002).

Forces exerted by blood flow play a clear role in AV specification, and also influence vessel morphogenesis and remodeling in the early embryo (Fang et al., 2017, Masumura et al., 2009, le Noble et al., 2004, Chong et al., 2011, Hwa et al., 2017). Hemodynamic force is both

necessary and sufficient to remodel the high-resistance mouse YS capillary plexus into a more complex hierarchical network with a large caliber VA and VV progressively leading to smaller diameter vessels (Lucitti et al., 2007). Our lab has shown that murine YS vessel remodeling depends on both vessel fusion and EC migration (Udan et al., 2013). Interestingly, live imaging studies showed distinct differences in how arterial and venous cells respond to changes in hemodynamic force (Udan et al., 2013, Kondrychyn et al., 2020, Goetz et al., 2014). These data suggest that pathways that control AV identity, which can be regulated by blood flow, may also influence physical responses of ECs to blood flow such as migration and motility that facilitate vessel remodeling.

Despite the knowledge gained regarding the mechanisms regulating arterial-venous identity and the discovery of mechanosensors that are required for ECs to sense blood flow, a full understanding of these mechanistic pathways is yet to be realized. A recent analysis estimates that approximately 6% of genes in the genome (~1200) may be required during early cardiovascular development (E9.5-E12.5) (Dickinson et al., 2016). One such gene, and the focus of this study, is *FoxO1 (Forkhead box protein O1)*. *Forkhead domain class O transcription factors* (*FOXOs)* integrate different cellular signaling pathways to regulate cellular homeostasis (Paik et al., 2007, Huang and Tindall, 2007, Jiramongkol and Lam, 2020). *Daf-16/FoxO* was originally identified as a regulator of dauer formation in *C. elegans* (Albert et al., 1981) and was later shown to control longevity by sensing environmental cues such as hormones, nutrient availability, oxidative stress, and energy metabolism via signaling through the insulin, AKT/mTor, JNK and AMPK pathways (Sun et al., 2017). Several studies have since established that *FoxO1* is also required for normal embryonic development in mice. Homozygous null *FoxO1* embryos display a primitive YS vasculature, pericardial edema, and disorganized embryonic vessels by E9.5, resulting in lethality by E11.5 (Furuyama et al., 2004, Dharaneeswaran et al., 2014, Hosaka et al., 2004, Sengupta et al., 2012, Wilhelm et al., 2016, Ferdous et al., 2011). Further analysis showed that *Tie2-cre* mediated loss of *FoxO1* in the

endothelium, but not the myocardium, phenocopied germline loss of *FoxO1* (Sengupta et al., 2012), demonstrating the requirement for FOXO1 in the embryonic vasculature. Follow-up studies have since found that FOXO1 controls a variety of different processes in endothelial cells (ECs), including, but not limited to EC proliferation and metabolism (Wilhelm et al., 2016), endothelial barrier function (Beard et al., 2020), sprouting angiogenesis (Kim et al., 2019, Fukumoto et al., 2018, Dang et al., 2017), autophagy (Zhang et al., 2019), EC growth (Riddell et al., 2018, Rudnicki et al., 2018) and migration (Niimi et al., 2017). Despite these studies, the exact function that FOXO1 plays in the early vasculature remains elusive. Given that FOXO1 activity can be modulated in response to fluid shear stress (Chlench et al., 2007, Dixit et al., 2008), combined with our studies showing that hemodynamic force is necessary and sufficient for early vascular remodeling (Lucitti et al., 2007, Udan et al., 2013), and the growing evidence for FOXO1 in cell migration and sprouting angiogenesis (Fosbrink et al., 2006, Niimi et al., 2017, Kim et al., 2019), we sought to define the requirement for FOXO1 in the remodeling vasculature of the early embryonic YS.

Herein, we demonstrate a novel role for FOXO1 in regulating AV identity in the murine YS vasculature. From conditional loss-of-function mutants, where *FoxO1* is deleted specifically in *Tie2-cre* expressing cells (predominantly ECs) (Eklund and Olsen, 2006, Schlaeger et al., 1997, Kisanuki et al., 2001, Chu et al., 2016), we identified a significant down regulation of arterial gene expression in the mouse YS prior to the onset of blood flow. We also detected a significant reduction in *Vegfr2/Flk1* transcripts, but normal expression levels for other pan-endothelial genes such as *Pecam1*, indicating that the formation of ECs is not disrupted but rather VEGF signaling is affected. Using a recently developed *Dll4* arterial reporter line (Herman et al., 2018), we showed that *FoxO1* is required for *Dll4* expression in the murine YS, but not in the embryo proper. Further analysis showed that FOXO1 represses expression of *Sprouty* genes, which encode inhibitors of Raf/MEK/ERK signaling downstream of FGF and VEGF receptor activation. Sprouty factors also modulate angiogenesis by negatively regulating small

vessel branching, as well as repressing EC migration (Gong et al., 2013, Wietecha et al., 2011, Lee et al., 2001). While some have shown that FOXO1 positively regulates *Sprouty* gene expression in the liver (Paik et al., 2007), our studies demonstrate that *FoxO1* loss increased *Sprouty2* and *4* mRNA levels, suggesting that FOXO1 represses *Sprouty2/4* in the murine YS. We went on to find that *Sprouty4* overexpression throughout the YS and embryo profoundly altered arterial gene expression in the YS but, similar to early FoxO1 loss, had an insignificant effect on these transcripts in the embryo proper. Taken together, these data highlight a novel role for FOXO1 in regulating arteriovenous specification in the early YS and reveal a new mechanism wherein FOXO1 represses *Sprouty* gene expression and downstream signaling in the endothelium.

Results:

YS vascular remodeling defects in *FoxO1*^{ECKO} embryos is not due to abnormalities in hemodynamic force or allantois defects

To define the role of FOXO1 in ECs within the early embryo, we conditionally ablated *FoxO1* in the endothelium by crossing female *FoxO1*^{flox} mice (Paik et al., 2007) with male *Tie2-Cre* transgenic mice giving control (*Tie2-Cre*$^{+/+}$*;FoxO*$^{+/flox}$) and CKO (*Tie2-Cre*$^{+/tg}$*;FoxO1*$^{flox/flox}$, hereafter referred to as *FoxO1*^{ECKO}) embryos, in which Cre recombinase is expressed in endothelial and hematopoietic cells and progenitors starting at E7.5 (Kisanuki et al., 2001). The efficiency of the *Tie2-Cre* mediated recombination of the *FoxO1*^{flox} allele was confirmed at the transcript level by qRT-PCR and at the protein level by western. We found at E8.5, *FoxO1* mRNA was significantly reduced in the conditional knockout YSs compared to control littermates, in contrast to the germline knockouts where *FoxO1* transcripts were undetectable (Figure 1A-C, and S1C). FOXO1 protein levels were also significantly reduced at E8.5 We observed gross phenotypes in *FoxO1* conditional and global knockout mutants similar to

previous reports (Figure 1D and E and S1A and B) (Sengupta et al., 2012, Furuyama et al., 2004, Hosaka et al., 2004). We did not detect any visible differences in vascular morphology or embryo size between control and *FoxO1*^{ECKO} at E8.5 (Figures 1F and G). However, at E9.5 and E10.5, while the primitive vascular plexus of the control YS remodeled into a hierarchy of large caliber vessels iteratively branching into smaller diameter capillaries, *FoxO1*^{ECKO} YSs retained a primitive vascular plexus (Figures 1H-K). *FoxO1*^{ECKO} YSs labeled with anti-PECAM1 (CD31) antibodies, a pan EC marker, showed normal plexus at E8.5 but thinner and less branched vitelline vein and artery compared to controls by E9.5 (Figure 1L-Q). At E9.5, mutant embryos were reduced in overall size compared to control littermates (Figures 1H and I), which became more evident at E10.5 (Figures 1D, E, J, and K). Additionally, in both E9.5 (not shown) and E10.5 *FoxO1*^{ECKO} embryos (Figure 1K), the pericardial sac was enlarged, and blood was abnormally pooled in the heart. Overall, phenotypes in *FoxO1* conditional and global mutant embryos are highly reproducible and our observations align well with previously published studies (Sengupta et al., 2012, Furuyama et al., 2004, Hosaka et al., 2004), supporting the conclusion that loss of *FoxO1* in ECs and other *Tie2* expressing cells is sufficient to cause defects in vessel remodeling.

The appearance of pericardial edema in *FoxO1*^{ECKO} embryos suggested heart failure and compromised circulation. To determine if and when blood flow was impaired, we crossed a primitive erythrocyte transgenic fluorescent reporter line, *ε-globin-KGFP* (Dyer et al., 2001) into the *FoxO1*^{ECKO} background. Live imaging of cultured embryos and high-speed confocal microscopy was used to track individual KGFP labeled erythroblasts to determine blood velocity (Figure 2) (Jones et al., 2004). At E8.5, both control and *FoxO1*^{ECKO} embryonic vessels were filled with blood and erythrocytes moved with a steady directional flow with similar periodicity and velocity (Figures 2A, B, E, and G). By E9.5, control embryos had clearly remodeled vessels, blood flow velocity greater than 700 μm/s, and a defined wave pattern with periodicity of 400 ms (Figures 2C and F). However, *FoxO1*^{ECKO} embryos vessels were not remodeled, and blood flow

had a significantly lower velocity with a poorly defined wave pattern (Figures 2D and H). Quantification of blood velocity (Figures 2I and J) and heart rate (Figures 2K and L) revealed no statistical difference in E8.5 control and *FoxO1*^{ECKO} embryos (Figures 2I and K). However, by E9.5, blood velocity and heart rate were significantly decreased in *FoxO1*^{ECKO} embryos (Figures 2J and L), indicating heart failure was occurring in embryos with un-remodeled vessels. Thus, flow initiates normally in *FoxO1*^{ECKO} embryos, but defects in both vascular remodeling and blood flow abnormalities were observed by E9.5. Given these results, we restricted our analysis, whenever possible, to E8.25 (4-7 somite range) embryos so that poor blood flow did not influence our data.

A previous report on the role of *FoxO1* in placental development described phenotypes including swollen or hydropic allantois, failed chorion-allantoic fusion, and increased cell death in the allantois (Ferdous et al., 2011). Since the previous study was conducted in germline *FoxO1* null embryos, we examined the allantois in global null and *FoxO1*^{ECKO} mutants. While germline *FoxO1* mutants exhibited partially penetrant defects in allantois formation and fusion, these phenotypes were not evident in *FoxO1*^{ECKO} embryos at E9.5 (Table 1). However, both germline and *FoxO1*^{ECKO} embryos show defects in YS vascular remodeling, heart failure phenotypes, and lethality by E11.5. Taken together, these results support a cell autonomous requirement for FOXO1 in YS vessel remodeling and suggest that published cardiac and blood flow defects are secondary to the impaired remodeling of YS vasculature.

FOXO1 is necessary to maintain *Flk1/Vegfr2* expression in E8.25 YSs

To assess mechanisms disrupted in *FoxO1*^{ECKO}, we examined transcript levels of genes normally expressed in blood vessels by qRT-PCR within *FoxO1*^{ECKO} E8.25 YSs. We focused these experiments at E8.25 prior to vessel remodeling and to avoid potential complications of later stage heart failure. We observed a significant decrease in *Flk1/Vegfr2* expression in *FoxO1*^{ECKO} YSs, while other pan-endothelial markers such as *Pecam1*, *Tie2*, *VE-Cadherin*,

Flt1/Vegfr1, and *Cx43* were not significantly affected (Figure 3A). Consistent down regulation of *Flk1/Vegfr2* was also seen in the *FoxO1* global knockout YSs and no change in *Flk1/Vegfr2* expression was detected in the embryo proper (Figure S2A). Immuno-labeling of endogenous *Flk1/Vegfr2* showed a similar reduction in expression in *FoxO1*^{ECKO} YS ECs at E8.25, while PECAM1 (CD31) expression appeared unaffected (Figure 3B). We further confirmed the reduction in *Flk1/Vegfr2* expression using magnetic-activated cell sorting (MACS) to isolate CD31^{+} cells (primarily ECs) from E8.25 WT and *FoxO1* germline deletion mutant YSs. CD31^{+} YS cells showed seven-fold higher *Pecam1* (CD31) expression than whole YSs (sorted then recombined) and approximately thirty-fold higher than the CD31^{-} population, demonstrating high fidelity enrichment via MACS (Figure 3C). To compare WT and mutant YS ECs, we assayed transcript levels of both *Pecam1* and *Flk1/Vegfr2* in the CD31^{+} populations. *Pecam1* levels were comparable between WT and mutant CD31+ cells, whereas *Flk1* was significantly reduced in the null CD31+ population (Figure 3D and E). Finally, we examined *Flk1* expression using a transgenic reporter, *Flk1-H2B::YFP* (Fraser et al., 2005), which labels EC nuclei. At E8.25, YFP^{+} endothelial nuclei were evenly dispersed throughout the vascular plexus of control YSs, however, the number of YFP^{+} nuclei within the *FoxO1*^{ECKO} YSs were significantly reduced (Figure 3F). The total number of DAPI^{+} nuclei was unchanged. Nuclear segmentation and quantification of the average YFP^{+} cell density revealed a significant reduction in the number of YFP^{+} cells in *FoxO1*^{ECKO} YSs compared to controls (Figure 3G). To determine if the reduction in YFP^{+} cells was due to a difference in apoptosis or proliferation, *FoxO1*^{ECKO} litters positive for the *Flk1-H2B-YFP* reporter were immunostained for phospho-histone 3 (PH3) or Caspase 3 (Figure 3H and I). We found that neither cell proliferation nor apoptosis within the YS differed significantly between control and *FoxO1*^{ECKO} embryos (Figures 3 H, I, S2B-E). Since the mRNA expression of pan-endothelial markers was not decreased, but Flk1 transcripts and protein were reduced, we concluded that the low density in YFP^{+} cells is not due to reduced EC numbers, but rather reduced expression of the *Flk1* reporter. Collectively, these data indicate that FOXO1 is

required to maintain cell autonomous *Flk1/Vegfr2* expression in ECs, but not required for the formation, proliferation or survival of ECs or the expression of other pan-endothelial markers.

FOXO1 is required to regulate arterial gene expression in the YS vasculature

Given the reduced *Flk1/Vegfr2* expression in E8.25 YSs, and the critical role of VEGF-VEGFR2 signaling in establishing arteriovenous identity in the early embryonic endothelium, we next examined other AV specification markers (Figure 4A). Previously, Furuyama *et al*. showed reduced arterial-enriched transcripts *Cx40, Cx37, eNOS, and EphrinB2* in E9.5 *FoxO1*^{ECKO} YSs compared to control littermates (Furuyama et al., 2004), but given the changes in blood flow that we observed in E9.5 *FoxO1*^{ECKO} embryos, we were interested to determine if expression of these markers was affected earlier. Indeed, these genes were significantly reduced in *FoxO1*^{ECKO} YSs at E8.25 compared to controls (Figure 4A). In addition, we found a significant reduction in Notch family members transcript levels, including *Notch1*, *Hey1*, *Jagged1* and *Dll4*, which are required for arterial specification (Gridley, 2010, Duarte et al., 2004, Xue et al., 1999, Fischer et al., 2004). Venous markers, *Neuropilin2 (NRP2), Coup-TFII (NR2F2)* and *EphB4*, showed no significant change (Wang et al., 1998, You et al., 2005). The endodermal marker *Afp* was also unchanged (Figure 4A) (Dziadek and Adamson, 1978). These results demonstrate that FOXO1 is required for normal early arterial gene expression in the murine YS.

To determine if reduced arterial-specific gene expression correlated with decreased expression of their respective proteins in *FoxO1*^{ECKO} YSs, immunofluorescence was performed on sectioned YSs at E8.5 and E9.5. Confocal imaging of Cx37 and Cx40 revealed an overall reduction in the number of connexin-positive puncta in *FoxO1*^{ECKO} YSs when compared to controls at both stages (Figure S3A and B). Similarly, we observed decreased eNOS expression within the vascular plexus in *FoxO1*^{ECKO} yolks sacs compared to controls (Figure 4B). These data, in addition to previous gene expression analysis, indicate that FOXO1 within the developing endothelium is necessary for the regulation of arterial identity.

Characterization of arterial defects in *FoxO1*^{ECKO} and germline mutants using the *Dll4-BAC-nlacZ* reporter

Thus far, our phenotypic, transcriptional, and immunolabeling studies support a role for FOXO1 in regulating vascular remodeling, *Flk1* expression, and arterial specification of ECs within the YS. To further analyze the arterial specification defects in *FoxO1*^{ECKO} mutants, we examined the spatial expression of one of the earliest markers of arterial identity (Chong et al., 2011, Wythe et al., 2013), *Dll4*, using a transgenic reporter line, *Dll4-BAC-nlacZ*, that faithfully recapitulates endogenous *Dll4* expression (Herman et al., 2018). E8.25 *FoxO1*^{ECKO} embryos carrying the nuclear-localized β-galactosidase reporter were compared with control littermates (Figure 5 and S4). In E8.25 control embryos, *Dll4-BAC-nlacZ* reporter activity was observed in the dorsal aorta (DA), endocardium (EN), and nascent umbilical artery (UA) within the allantois (Figure 5A and S4A). LacZ positive nuclei were also detected within the YS in and around the vitelline artery and arterioles (Figure 5A, red arrows). *FoxO1*^{ECKO} YSs exhibited a similar LacZ expression pattern spatially, albeit with reduced intensity (Figure 5B), consistent with our transcript analysis showing reduced *Dll4* mRNA expression in the *FoxO1*^{ECKO} YSs (Figure 4A and 5C). However, unlike in the YS, nLacZ expression was only slightly reduced in the embryo proper of *FoxO1*^{ECKO} mutants (Figure S4B compared to S4A, Figure 5C). To determine if the differences in nLacZ reporter expression between the YS and embryo was influenced by Cre-mediated recombination in our conditional knockout studies, we examined the activity of the *Dll4* LacZ reporter in germline *FoxO1* mutants. Figures 4SE and F show representative images of anterior views of the embryos, while Figure 5D and E show posterior views. *FoxO1*$^{null/null}$ showed even greater decreases in reporter expression compared to control YSs and embryos (5D and 5E red arrows). A small, but significant decrease in endogenous *Dll4* expression was seen between WT and *FoxO1* $^{null/null}$ embryos (Figure 5F). Whereas, a dramatic reduction in *Dll4* expression was observed in the *FoxO1* null YSs compared to wildtype controls (Figure 5F).

By E9.5, nLacZ reporter expression was detected in the arterial tree in the YS, particularly in the VA and within the arterioles (Figure 5G and 5G inset). Consistent with the E8.25 results, we found *Dll4* expression reduced in E9.5 *FoxO1*^{ECKO} YSs (Figure 5H and 5H inset) but strong expression in vessels within control and *FoxO1*^{ECKO} embryos (Figures 5I and J). Germline null embryos showed similar nLacZ activity compared to controls (Figure 5K), but reporter expression was not detectable in null YSs, despite the strong expression seen in the embryo (5L). Isolated embryos confirmed LacZ expression in both control (5M) and null embryos (5N). Additional analysis of *Dll4* reporter expression confirmed previous reports of vascular defects in *FoxO1* mutants, including within the intersomitic vessels, cranial vessels and dorsal aorta (5I, J,M, and N, red arrows) (Hosaka et al., 2004, Ferdous et al., 2011, Dharaneeswaran et al., 2014). Collectively, our results indicate that FOXO1 plays a critical and early role in the regulation of *Dll4* expression, a key factor in determining arterial identity, within the extra-embryonic arteries of the YS, but does not appear to be required for *Dll4* expression within the embryo proper.

Conditional *FoxO1* deletion upregulates *Sprouty2l4* expression

We uncovered a novel role for FOXO1 in the establishment of arterial identity, but neither *Flk1* nor *Dll4* contain known binding sites for FOXO1, thus we examined expression levels of previously validated, direct transcriptional targets of FOXO1 in the endothelium: adrenomedullin (*Adm)*, BMP binding endothelial regulator (*Bmper*), *eNOS*, *Sprouty2*, and *Vcam1* (Potente et al., 2005, Ferdous et al., 2011). qRT-PCR analysis in *FoxO1*^{ECKO} YSs at E8.25 (Figure 6A) revealed no significant reduction in *Adm* or *Bmper,* but a significant downregulation in *eNOS* and *Vcam1* compared to controls, as previously described in other tissues (Potente et al., 2005, Ferdous et al., 2011). Interestingly, *FoxO1*^{ECKO} YSs showed significantly increased *Sprouty2* expression (Figure 6A). Subsequent analysis showed that in addition to *Sprouty2*, *Sprouty4* was also upregulated in mutant YSs compared to controls, while *Sprouty1* and *3* levels were unchanged

(Figure 6B). The upregulation in *Sprouty2* and *Sprouty4* is specific to the YS as no significant changes in *Sprouty* expression were seen in the embryo proper (Figure S5). We focused our subsequent analysis on the Sprouty factors because Sprouty4 over-expression has been shown to inhibit angiogenesis in the YS (Lee et al., 2001) and the upregulation of *Sprouty* transcripts in *FoxO1*^{ECKO} led us to hypothesize that FOXO1 may act as a direct repressor of *Sprouty* gene expression.

In keeping with the idea that FOXO1 may normally repress *Sprouty 2/4* transcription, we examined endogenous mRNA levels of *FoxO1* and *Sprouty1-4* in wildtype E8.25-8.5 YSs. This analysis revealed that *Sprouty2/4* expression is much lower than *FoxO1*, *Sprouty1* or *Sprouty3* (Figure 6C). To expand and confirm endothelial specificity of our previous *Sprouty 2/4* expression analysis, we examined *Sprouty 2/4* transcripts in CD31^{+} and CD31^{-} MACS-sorted cells from germline *FoxO1* mutants and WT YSs (Figure 3D). For *Sprouty2*, we observed increased expression in YS CD31^{+} cells, but there was no change in CD31- cells from null mutant YSs (Figure 6D). Surprisingly, while *Sprouty4* transcripts were increased in CD31+ cells of null YSs, transcripts were decreased in the CD31- population. These data suggest that FOXO1 may act as both a transcriptional repressor or activator in adjacent tissues in the YS, depending on the cell identity or transcriptional target.

FOXO1 directly binds to endogenous *Sprouty2/4* promoters and represses *Sprouty2/4* transcription

FOXO1 is known to regulate *Sprouty2* mRNA expression in liver ECs, and *in vivo* chromatin immunoprecipitation (ChIP) experiments confirmed that FOXO1 occupies four conserved FOXO binding elements within the murine *Sprouty2* locus (Paik et al., 2007). The first FOXO1 binding site (Figure S5A) is located ~4kb upstream of the transcriptional start site (TSS) of murine *Sprouty2,* and the second DNA-binding site is within exon 2 (Figure 7A). The third and fourth FOXO1 binding sites are located ~5kb and 7kb downstream of the TSS, respectively (Figure

7A). Paik, et al. showed that FOXO1 interacts with these loci to activate *Sprouty2* in the liver, but it was unknown whether FOXO1 utilizes the same binding sites to repress *Sprouty2* in the YS. To determine if FOXO1 occupies any of these four identified binding sites in the murine YS, we performed ChIP-PCR using pooled WT E8.25 YSs. As shown in Figure 7B, FOXO1 occupancy was significantly enriched at the -4051, +5060, and +6972 regions compared to IgG control. FOXO1 enrichment was not observed at the +4479 region. This demonstrates that during early YS vessel development, FOXO1 binds *Sprouty2* at regulatory regions -4051, +5060, and +6972 and supports the context-dependent function of FOXO1.

Next, we generated luciferase reporter constructs containing ~2kb of the murine *Sprouty2* promoter, or specific regulatory regions harboring FOXO1 binding sites, and measured transcriptional activity in cultured mammalian cells (Figure S6B). To avoid potential confounds in our analysis from endogenous FOXO1, the human lung cancer cell line H1299 was chosen since FOXO1 protein expression is undetectable in this line (Zhao et al., 2010). Overexpression of *FoxO1* (*FLAG::FoxO1*) significantly repressed luciferase activity of the promoter construct containing the -4051 FOXO1 binding site in a dose dependent manner. Furthermore, co-transfecting the same reporter construct along with a FOXO1 cDNA without a DNA binding domain abolished this transcriptional repression (Figure 7C). In contrast, FOXO1 did not significantly repress luciferase activity in the constructs containing either the +4479/5060 combined or +6972 *Sprouty2* regulatory regions (Figure 7C). These results suggest that FOXO1 directly downregulates *Sprouty2* expression via the -4051 site in its promoter.

To determine if this role for FOXO1 is evolutionarily conserved, we examined the *Sprouty4* locus for conserved FOXO1 DNA-binding motifs (Figure S6A). Two putative binding sites, which were conserved in at least three vertebrate genomes (mammalian and non-mammalian), were identified +8755 bp and +14942 bp downstream of the *Sprouty4* TSS (Figure 7D). FOXO1 ChIP-PCR using E8.25 YS chromatin showed a significant enrichment

of FOXO1 occupancy in both regulatory regions (Figure 7E). Luciferase assays in H1299 cells also showed that these same sites were required for wildtype FOXO1 dose-dependent repression of reporter activity (Figure 5F and S6C). Taken together, data from the *Sprouty* mRNA expression analysis, as well as ChIP and luciferase assays, demonstrated that FOXO1 directly repressed *Sprouty2* and *Sprouty4* transcription in the E8.25 murine YS via known and newly identified conserved DNA-binding sites.

Transient overexpression of *Sprouty4* in ECs partially phenocopies conditional loss-of-function *FoxO1* mutants

Sprouty2 and *Sprouty4* are known to have anti-angiogenic functions (Taniguchi et al., 2009, Wietecha et al., 2011, Lee et al., 2001), and our data here show that FOXO1 directly represses *Sprouty2/4* expression in the YS, we hypothesized that FOXO1 promotes arterial gene expression by repressing *Sprouty2/4.* It had previously been shown that adenovirus-mediated overexpression of *Sprouty4* in developing embryos inhibited sprouting and branching of small vessels in the embryo proper and vessel remodeling in the YS (Lee et al., 2001). To test whether *Sprouty4* overexpression could recapitulate the *FoxO1* loss-of-function phenotype, we utilized a well-characterized *Flk1* promoter-enhancer construct that is expressed in YS and embryonic ECs (Kappel et al., 1999, Ronicke et al., 1996, Fraser et al., 2005) to transiently overexpress *Sprouty4* beginning at E7.5. To track transgene expression, a H2B::YFP reporter was inserted downstream to enable YFP^+ transgenic embryo identification (schematized in Figure 8A). At E9.5 YSs of YFP^+ transgenic embryos (n=3) showed poorly remodeled vasculature, as their vessels remained as a primitive vascular plexus, while non-transgenic embryos had a normally developed vitelline artery with large caliber vessels branching into smaller diameter capillaries (Figure 8B). The lack of YS vascular remodeling in the transient transgenic *Flk1-Sprouty4* embryos phenocopied the vascular remodeling defects in $FoxO1^{ECKO}$ embryos and was similar to previous loss of function data (Lee et al., 2001). YSs harvested from

both transgenic and control embryos confirmed the expression of YFP transcripts and exogenous *Sprouty4* only in transgenic embryos (Figure S7).

Next, we utilized total RNA from transgenic YFP^+ and control YSs and embryos that were within E8.25 4-7 somite stage for analysis. The relative expression level of each arterial marker was first normalized *Gapdh*, the internal control, then to endogenous *Sprouty4* in order to compare the effect of exogenous *Sprouty4* overexpression. Transcript levels were compared between control and YFP^+ transgenic groups. Arterial markers, such as *Cx37*, *EphrinB2*, *Notch1*, *Hey1*, *Jagged1*, and *Dll4* were significantly downregulated in the YSs of transgenic embryos compared to controls (Figure 8C), while expression within the embryo proper of these markers was not significantly changed, apart from *Jagged1* (Figure 8D). *Cx40* expression was not significantly different between the control and transgenic groups in either the YS or embryos (Figures 8C and D). Additionally, unlike in *FoxO1*^{ECKO} YSs, expression of venous marker *EphB4* was significantly down regulated in the YS and *Coup-TFII* expression was significantly increased in the transgenic embryos. The broader effects produced by *Sprouty4* overexpression directed by the *Flk1* promoter/enhancer could indicate that Sprouty4 has FOXO1 independent functions, or that abnormally high levels of *Sprouty4* may affect other processes. These data, combined with our results showing that FOXO1 represses *Sprouty2/4* transcription, indicates that FOXO1 acts as a key transcriptional regulator in arterial-venous specification by repressing an antagonist of arterial specification.

DISCUSSION

Previously, using either germline mutations or conditional approaches, several groups demonstrated a requirement for FOXO1 in the early embryo, as these mutants featured failed YS remodeling and mid-gestation lethality (Sengupta et al., 2012, Furuyama et al., 2004, Hosaka et al., 2004). In this paper, we investigated the role of FOXO1 within the YS vascular plexus prior to the onset of consistent circulation and overt vascular remodeling. It is well known

that arteriovenous specification and the arterial gene expression program are influenced by hemodynamic forces (le Noble et al., 2004, le Noble et al., 2005, Wragg et al., 2014), but our goal here was to determine whether FOXO1 functions before the onset of hemodynamic signaling to affect arteriovenous patterning. Herein, we demonstrate that blood flow is normal in *FoxO1*^{ECKO} mutants at these early stages, although heart failure and poor circulation are evident by E9.5 (Figure 2). Others have shown that FOXO1 is not required for heart development (Sengupta et al., 2012), and it is possible that heart failure in these embryos is caused by the increased resistance of blood flow encountered in the unremodeled vitelline vessels. Additionally, loss of FOXO1 causes allantois defects, preventing normal allantois fusion and circulation to the placenta (Ferdous et al., 2011). We did not observe overt defects in allantois fusion in *FoxO1*^{ECKO} embryos (0/10 *FoxO1*$^{flox/flox}$*;Tie2-cre*$^{Tg/+}$) (Table 1) and observed only low penetrance of allantois fusion defects in (2/15) in the germline *FoxO1* knock out embryos, whereas 100% of all null or *FoxO1*^{ECKO} embryos examined showed defects in YS remodeling, heart failure and mid-gestation lethality. Thus, it is likely that the heart failure and lethality are caused by increased resistance to blood flow in vitelline vessels; however, the reduction in *Dll4* expression that we observed using the *Dll4-BAC-nlacZ* reporter in *FoxO1*^{ECKO} and germline null mutants suggest that further investigation of the consequence *Dll4* loss in allantois development is warranted.

In this study, we report that FOXO1 plays a previously unidentified role in regulating arterial-specific gene expression prior to the onset of blood flow. Based on transcript expression analyses, immunostaining, and transgenic reporter experiments, we have concluded that loss of *FoxO1* causes a significant downregulation in *Flk1* and critical arterial markers, including *Dll4*, in the YS without affecting cell proliferation or cell death. Further, our data demonstrate that FOXO1 directly binds to *Sprouty 2* and *4* regulatory regions in the YS, and that FOXO1 acts as a direct repressor of *Sprouty 2* and *4* in YS cells. Finally, we show that overexpression of *Sprouty4* in ECs *in vivo* was sufficient to recapitulate impairments in both vascular remodeling at

E9.5 and arterial cell fate specification at E8.25 seen in *FoxO1* mutants. These data, combined with our results showing that FOXO1 represses *Sprouty2/4* transcription, indicates that FOXO1 acts as a key transcriptional regulator in arterial-venous specification by repressing an antagonist of arterial specification. However, given the caveat that we also observed disruptions to venous marker expression in *Sprouty 4* overexpression embryos, it is not yet clear whether Sprouty factors only participate to limit arterial gene expression or if they play a broader role in early EC-specification.

Our studies support a model where FOXO1 represses *Sprouty2/4* in YS ECs to promote early, arterial specification in the YS prior to the onset of robust embryonic circulation. Interestingly, although we observed elevated *Sprouty 2/4* transcripts in YS CD31+ cells of *FoxO1* null, we found reduced *Sprouty 4* mRNA expression in CD31- cells in the YS, suggesting FOXO1 may act as activator for *Sprouty 4* in other cell types of the YS. Recent studies showed that FOXO1 functions as a transcriptional repressor in hepatocytes (Langlet et al., 2017) and pancreatic progenitor cells (Jiang et al., 2017). In some instances different co-factors have been identified that enable FOXO1 to act as an activator or a repressor in different cell types of the same tissues (Langlet et al., 2017). A similar mechanism may explain the observed differences between endothelial and non-ECs within the YS. It is not yet known whether a transcriptional co-factor in YS ECs is required for FOXO1 to act as a repressor, or if another mechanism accounts for the opposite regulation of *Sprouty 4* in adjacent cell layers. It is also not yet clear whether the down-regulation of *Sprouty* 4 in the CD31- cells has a functional consequence. Further work is needed to determine if Sprouty factors play multiple roles in early yolk sac development.

FoxO1 loss did not appear to effect normal expression of pan-endothelial markers *Pecam1*, *Tie2*, and other genes, but *Flk1/Vegfr2* was significantly reduced in both *FoxO1*^{ECKO} YS and sorted germline mutant YS CD31+ cells. We also found that despite the reduction in *Flk1/Vegfr2*, we did not observe changes in cell proliferation or cell viability, two process that are directly regulated by VEGF-VEGFR signaling (Bernatchez et al., 1999). Sprouty factors inhibit

receptor tyrosine kinase signaling, and Sprouty overexpression could cause a reduction in *Flk1/Vegfr2* that is normally promoted by FLK1 or FGF receptor activation (Lee et al., 2001, Casci et al., 1999). Indeed, we observed a reduction in *Flk1* transcripts when *Sprouty4* was overexpressed in transgenic embryos, but also observed a strong effect on the expression of other endothelial markers such as *Pecam1*. It is also possible that reduction of *Flk1* expression seen in *FoxO1* mutants is a secondary consequence of disrupted arterial specification, rather than a primary driver of this defect.

Dll4 is among the earliest markers of arterial gene expression (Chong et al., 2011, Wythe et al., 2013), but precisely how *Dll4* expression is initiated within the early YS and embryo remains poorly understood. While *Dll4* transcription was suggested to be regulated by 5' binding of FOXC1/2 and β-catenin in its proximal promoter (Corada et al., 2010, Hayashi and Kume, 2008, Seo et al., 2006), subsequent *in vivo* analysis showed that this region is not sufficient to mediate expression (Wythe et al., 2013). Additionally, endothelial-specific loss of *β-catenin* failed to alter *Dll4* expression in mice, or produce arteriovenous patterning defects (Wythe et al., 2013). Furthermore, functional enhancers were found within intron 3 and upstream at -12 and -16 kb that recapitulated the pattern of endogenous *Dll4* expression (Sacilotto et al., 2013, Wythe et al., 2013), and these regions lacked conserved FOXC1/C2 binding sites, as well as TCF/LEF binding sites. In these current studies, we used a nuclear localized LacZ reporter that recapitulates the normal expression pattern of *Dll4* (Herman et al., 2018). The data presented here clearly show that *FoxO1* is required to sustain *Dll4* and arterial gene expression through the repression of *Sprouty 2 and 4*, but there are likely other mechanisms involved in activation of *Dll4* and arterial gene expression.

Our data clearly showed that the reduction in *Dll4* expression was far more severe in the *FoxO1*^{ECKO} or null YS than within the embryo proper. In addition to *Dll4*, reduced *Flk1* expression (Fig S2 A) and alterations to *Sprouty 2/4* expression (S5 A) also appeared to be confined to the YS. Similarly, *Sprouty4* overexpression throughout the embryo and YS using an

endothelial-specific *Vegfr2/Flk1* promoter (Kappel et al., 1999, Ronicke et al., 1996, Fraser et al., 2005) indicated that *Sprouty* overexpression did not alter arterial gene expression in the embryo, but suppressed arterial transcripts (and altered some venous marker expression) in the YS. The mechanism that explains the differential activity of FOXO1 and SPROUTY2/4 within the vasculature of the YS vs the embryo proper remains unclear. Future experiments will be required to address numerous possible explanations including differences in mesodermal cell lineages, differential binding to cofactors and/or differences in post-translational modifications regulated by local cell-cell signaling.

One unresolved question from these studies is the relationship between abnormal arteriovenous specification and failed vessel remodeling. Both arteriovenous identity and vessel remodeling are regulated by hemodynamic forces, and AV specification relies on pathways that respond to VEGF signaling (Fish and Wythe, 2015, Covassin et al., 2006, Weinstein and Lawson, 2002, Fang et al., 2017). In *FoxO1*^{ECKO}, we detected downregulation of Flk1/VEGFR2. VEGFR2 and other VEGF receptors have been shown to act as shear stress mechanosensors, signaling through downstream pathways such as the MEK-ERK kinase cascade in response to changes in blood flow (Tzima et al., 2005, Baeyens and Schwartz, 2016). Thus, the downregulation of VEGFR2 in *FoxO1* mutant embryos could prevent ECs from responding to normal blood flow signaling needed for vessel remodeling. Previously, our lab showed that ECs within the vitelline arteries, but not the vitelline veins, migrate directionally in response to hemodynamic changes in YS vasculature (Udan et al., 2013) so it is possible that the loss of FOXO1 and/or the overexpression of *Sprouty2/4* interferes not only with initial *Dll4* specification, but with the cell's ability to sense mechanical signaling that is necessary to direct cell migration required for remodeling. Further work will be needed to better understand the mechanisms leading both to early *Dll4* expression and those that regulate the cellular responses needed for vessels to adapt to changes in blood flow.

EXPERIMENTAL PROCEDURES

Animals and genotyping

All animal experiments were conducted according to protocols approved by the Institutional Animal Care and Use Committee of Baylor College of Medicine. *Ella-Cre* and *Tie2-Cre* transgenic mice were purchased from Jackson Labs (# 003724 and 008863, respectively). *ε-globin-KGFP* (Dyer et al., 2001), *FoxO1*$^{flox/flox}$ mice (Paik et al., 2007), and *Dll4-BAC-nLacZ* mice (Herman et al., 2018) were maintained and genotyped as previously described. *FoxO1* germline knockout mice were generated by crossing the *FoxO1*$^{flox/flox}$ mice to *Ella-Cre* mice (Lakso et al., 1996). *Flk1-H2B::YFP* reporter mice were kindly provided by Dr. K. Hadjantonakis, Memorial Sloan Kettering Cancer Center (Fraser et al., 2005).

Immunostaining of whole or sectioned YSs

E8.25 YSs were fixed in 4% PFA, rinsed in PBS, permeabilized with 0.1% TritonX-100 for 1 hour, and blocked in 2% normal donkey serum/1% BSA for 5 hours. YSs were then incubated with anti-PECAM1 antibody (BD Pharmingen, #550274; 1:100) overnight at 4°C. After several PBS washes, YSs were incubated with goat anti-rabbit antibody (Molecular Probes, AlexaFluor 633,1:500) and DAPI (1:500) overnight at 4°C. Finally, YSs were rinsed in PBS and imaged using the Zeiss LSM510 META confocal microscope. Dissected YSs were cryosectioned at 20μm and sections were permeabilized and blocked, and incubated with antibodies to either Caspase 3 (Cell Signaling #9661, 1:50); Connexin37 (ThermoFisher Scientific #404200, 1:50); Connexin40 (ThermoFisher Scientific #364900, 1:50); eNOS (Santa Cruz #sc-654, 1:50); Flk1 (Sigma #V1014, 1:100); or pHistone H3 (Millipore #06-570, 1:50) overnight at 4°C. The secondary antibody incubation and image acquisition were performed as described previously.

LacZ staining

Dll4-BAC-nLacZ transgenic reporter were examined on *FoxO1* germline or *FoxO1*^{ECKO} (*Tie2-Cre*$^{+/tg}$;*FoxO1*^{floxflox}) backgrounds. E8.5 and E9.5 embryos were dissected in cold PBS and fixed in 4% PFA. Embryos were then washed in X-gal rinse buffer (0.02% NP40, 0.01% sodium deoxycholate; 4 x 15mins) and thereafter stained in x-gal solution [5mM $K_3Fe(CN)_6$, 5mM $K_4Fe(CN)_6$, 0.01% sodium deoxycholate, 0.02% NP40, 2mM $MgCl_2$, 5mM EGTA, 1mg/ml X-gal] at 37^{o}C overnight. Embryos were then post-fixed in 4% PFA and then cleared in 50% and 70% glycerol. Embryos from the same litter were processed and stained in a 20ml scintillation vial. Stained embryos were photographed using the Axio ZoomV16 (Zeiss) stereo microscope and thereafter genotyped.

Protein isolation and Western Blotting

Yolk sacs from three E8.25 WT or *FoxO1*^{ECKO} embryos were pooled and lysed in RIPA buffer (10mM Tris-HCl, pH 8; 1mM EDTA; 1% Triton X-100; 0.1% sodium deoxycholate; 0.1% SDS; 140mM NaCl; 1mM PMSF) supplemented with protease inhibitors. Protein lysates were quantitated using Bradford assay. Twenty micrograms of lysates were electrophoresed on 4-15% protein gels (Biorad), transferred to PVDF membrane, and immunoblotted with antibodies to either FOXO1 or GAPDH (Cell Signaling Technology, #2880 and 97166) overnight at 4^{o}C. After incubation with HRP conjugate secondary antibodies for an hour at room temperature, protein bands were detected via chemiluminescence with Clarity ECL western substrate (Biorad) on film. Western bands were quantified using Fiji gel analyzer and FOXO1 was normalized to GAPDH.

Quantification of *Flk1-H2B::YFP*$^{+}$ cell density, proliferation index and apoptotic index in whole mount YSs

Acquired WT and ECKO YS whole mount images (n>3 YSs per genotype, n>3 regions of interest per YS) were made into maximum intensity projections and separated into individual RGB images: Red (pHistone-H3/Caspase 3), Green (Flk1-H2B::YFP) and Blue (DAPI). Individual nuclei for RGB channels were segmented and quantified using FARSIGHT. FARSIGHT is an open source, image analysis tool box for segmentation and quantitation of biological features courtesy of Badri Roysam, University of Houston PMID: 18294697; https://github.com/RoysamLab/Farsight-toolkit). We used this to generateboth intensity and volume thresholds to distinguish two nuclei as separate. YFP^{+} cell density was defined as the ratio of YFP^{+} nuclei to DAPI^{+} nuclei within that same field of view. Proliferative/apoptotic index was defined as the ratio of PH3^{+}/ Caspase3^{+} nuclei to the number of DAPI^{+} nuclei. EC proliferative/apoptotic index was defined as the ratio of YFP^{+};PH3^{+}/Caspase3^{+} double positive nuclei to the number of YFP^{+} nuclei. The ratios were then averaged over the various WT and ECKO YS images.

Live imaging and analysis of blood flow in *FoxO1* conditional knockout embryos

ε-globin-KGFP reporter expressing GFP in primitive erythroblasts was examined in control and ECKO background and litters were dissected at E8.5 or E9.5 for blood velocity analysis. Embryos were dissected under a heated (37°C) dissection stage with warm dissection media (DMEM/F-12, 10% FBS, 100 U/mL penicillin, and 100 µg/mL streptomycin). Embryos with intact ectoplacental cone were placed in a glass bottomed culture chamber with culture medium (1:1 DMEM/F-12: rat serum, 100 U/mL penicillin, and 100 µg/mL streptomycin) and allowed to recover in a 37°C incubator for 20 minutes. Embryos were then placed on a heated confocal microscope stage (37°C) and imaged using the Zeiss LSM 5 LIVE laser scanning confocal

microscope, using the Achroplan 20X/0.45 NA objective. A 200-frame time lapse (in a 512x512 pixel frame) was acquired at 30-50 frames per second. Blood flow time lapses were acquired at three different locations throughout the YS per embryo, and at least three embryos of each genotype were used for data collection. Individual blood cell velocities in each track were determined from time lapse movies using Imaris. Individual blood cell velocities from three different locations per embryo were averaged. Average heart beats per minute were calculated by measuring the average time interval between peak velocities during the course of 5 cardiac cycles in individual velocity profiles for each embryo imaged. Embryos were genotyped after imaging, and blood velocities and heart beats per minute were averaged within WT and ECKO.

Magnetic activated cell sorting of YS ECs

To isolate E8.25 YS ECs, fresh YSs were dissected in cold DMEM/F12 media without phenol red (ThermoFisher Scientific #21041025), individually placed in 100 μL of cold TrypsinLE (Fisher Scientific #12605010), and kept on ice until all YSs were harvested. Embryos were used for genotyping. To dissociate YSs into single cell suspension, gently triturate with p200 pipette and incubate on ice for 5 minutes and repeat for a total of four times. To inhibit the enzyme, add 1 mL of stop solution: media + 10% FBS (ThermoFisher Scientific #26140079). The YS cell suspensions were pelleted at 0.8 X 1000g for 5 minutes at 4 degrees Celsius. The pellets were resuspended in 90 μL of cell suspension buffer (PBS + 2% FBS + 2 mM EDTA). 10μL of CD31 MicroBeads (Miltenyi Biotec #130-097-418) were added to each YS cell suspension and samples were incubated on ice for 15 minutes in the dark. Cell mixtures were pelleted at 0.8 X 1000g for 5 minutes at 4 degrees Celsius and washed with 1mL of cell suspension buffer. Cell mixtures were once again pelleted at 0.8 X 1000g for 5 minutes at 4 degrees Celsius and resuspended in 200uL of cell suspension buffer. Cell mixtures were passed through 40 μm cell strainers (Fisher Scientific #352340) into FACS tubes and strainers were washed with 300 μL of

cell suspension buffer. MS columns (Miltenyi Biotec #130-041-301) were placed on OctoMACS separator and prepared according to manufacturer instructions. Cell mixtures were individually passed through columns and the flow through was reapplied through columns to maximize EC retention ($CD31^+$ population). Columns were washed three times with 500 μL cell suspension buffer and all flow through was collected ($CD31^-$ population). Bound cells were released from the columns by removal from magnetic separator, and 1 mL of cell suspension buffer was applied to the columns and cells were flushed using plunger into a 1.5 mL Eppendorf tube. Collected cells were then pelleted at 0.8 X 1000g for 5 minutes at 4 degrees Celsius and resuspended in Trizol (Thermo Fisher 15596018). After genotyping, $CD31^+$ and $CD31^-$ populations from two YSs were combined and processed for RNA isolation (QIAGEN RNeasy Micro Kit #74004), cDNA synthesis and qRT-qPCR as described below.

RNA isolation and qRT-PCR analysis

Total RNA was isolated from pooled (2-8 YS/sample) E8.25 YSs dissected from either *Tie2-Cre*$^{+/tg}$*; FoxO1*$^{+/flox}$ or *Tie2-Cre*$^{+/tg}$*; FoxO1*$^{flox/flox}$ embryos. Purified RNA was reverse transcribed (ThermoFisher Scientific #11752-050) and gene expression analysis was performed using TaqMan real-time assays for *FoxO1*, *Adm, Bmper, Vcam1*, and a panel of endothelial, arterial, and venous markers (see Fig. 2D, E for gene list). The data were normalized to *Gapdh* (Pfaffl, 2001) and relative expression ratios between control and ECKO embryos were determined. Endogenous *FoxO1* and *Sprouty*1-4 expression from pooled E8.25 YSs (CD1 strain) was also probed by TaqMan real-time assay, but expression was calculated as fold change relative to *FoxO1*.

Endogenous *Dll4* expression was measured in either germline *FoxO1* knockouts or *FoxO1* ^{ECKO} embryos at E8.25. The allantois was used for genotyping and total RNA was extracted from individual embryos and YSs ($n \geq 3$) and probed for *Dll4* expression via TaqMan assay and fold

change of expression between controls and homozygous *FoxO1* ^{ECKO} mutants. Unpaired student's *t* -test was used to assess statistical significance and *P* values <0.05 were considered statistically significant.

Chromatin Immunoprecipitation (ChIP) and qPCR

To determine endogenous FOXO1 chromatin occupancy, E8.25 YSs from CD1 embryos were used for chromatin extraction. Freshly dissected YSs were dissociated in ice cold PBS with protease inhibitors and the tissue was then crosslinked with 1.5% formaldehyde, followed by incubation with 125 mM glycine, and washed with PBS. After centrifugation, the pellet was resuspended in cell lysis buffer (5 mM PIPES, pH 8; 85 mM KCl; 0.5% NP40). The samples were spun and the pellet was resuspended in nuclear lysis buffer (50 mM Tris-HCl, pH 8.1; 10 mM EDTA; 1% SDS) and then sonicated on ice using a Bioruptor (Diagenode) to obtain sheared chromatin ranging between 100–500 bp. ChIP was performed according to the instructions for Magna ChIP kit (Millipore #17-10085) using 5 µg of anti-FOXO1 antibody (Abcam #ab39670) or rabbit IgG (Millipore #12370). The cross links were then reversed, and the purified DNA was then analyzed by qPCR in technical triplicates using SYBR green master mix and the primers listed in Table S1 to measure the percentage of co-precipitating DNA relative to input (% input) in *Sprouy2* and *Sprouty4* genomic regions.

Cloning of *mSprouty2/4* promoter constructs and Luciferase Assay

Genomic regions of ~2kb in length of murine *Sprouty2* and *Sprouty4* were PCR amplified using primers listed in Table S1and using BAC clones of C57BL6 genomic DNA as template DNA (CH29-611D15, CH29-100M12, respectively; CHORI BAC/PAC resources). PCR fragments were ligated into pCRII-TOPO vector, sequenced, and then subcloned into pGL3-Promoter vector (Promega). H1299 cells (ATCC #CRL-5803) were maintained in DMEM media supplemented with 10% FBS, 100 U/ml penicillin, and 100 µg/ml streptomycin. For transient

transfections, 50,000 cells were plated (48-well plate) and after 24 hours, each well was co-transfected with 200 ng of *Sprouty2/Sprouty4* promoter construct, 10 ng of pRL-TK, and 125 ng expression plasmid (pcDNA3-FOXO::FLAG, Addgene #13507) using manufacturer's recommendations for lipofectamine 3000. The total amount of expression plasmid transfected per well was kept constant with varying amounts of pcDNA3.1 vector. As a negative control, a *FoxO1* plasmid encoding a deleted DNA binding domain (amino acid 208-220) was used (Addgene #10694). After 24 hours, cells were lysed and analyzed for firefly and *Renilla* luciferase activities according to the procedure outlined in the Dual-Glo luciferase assay system (Promega #E2920). All luciferase assays were performed in triplicates and repeated at least three times. Student's *t* -test was used to assess statistical significance ($P < 0.05$ was considered statistically significant) and the averages and standard deviation from triplicate samples from representative assays were shown.

Transient endothelial-specific *Sprouty* expression in embryos

A mouse *Sprouty4* cDNA clone (TransOmics clone BC057005) was used as a template to PCR amplify the coding sequence with 5' *Sac*I and 3' *Pme*I restriction sites (5' GAGCTCCCAGCCTCA TGGAGCCC 3' and 5' GTTTAAACTCAGAAAGGCTTGTCAGAC 3') and subcloned into pCRIITOPO vector (S4-2). The internal ribosome entry site (IRES) sequence was amplified from pIRES-hrGFP1a vector (Agilent Technologies) with 5' *EcoR*V and 3' *EcoR*I restriction sites using primers 5' CTATAGATATCACCCCCCTCTCCCTA 3' and 5' GCATGAATTCGGTTGTGGCCATT ATCATCGTG 3' and subcloned into pCRIITOPO vector (IRES-4). To assemble the final transgenic construct, clones S4-2 and IRES-4 were excised with 5' *Ecl136*II and 3' *Not*I, and 5' *Not*I and 3' *Ecl136*II, respectively, and co-ligated into *Flk1*-H2B/EYFP vector (kindly provided by Dr. K. Hadjantonakis, Memorial Sloan Kettering Cancer Center) via a blunt-ended *Hind*III site. The *Flk1*-H2B/EYFP vector has a well characterized *Flk1* promoter and intronic enhancer sequences which drive YFP expression in ECs (Fraser et al.,

2005). All clones were verified by DNA sequencing and the final transgenic construct was excised with 5' *Sal*I and 3' *Xba*I to purify a 4.5kb fragment for pronuclear microinjection, which was performed at the BCM Genetically Engineered Mouse Core. Transient transgenic embryos were dissected with YS intact and initially screened for YFP expression using confocal microscopy. Gross morphology of the embryo and YS vasculature was examined at E9.5 while arterial marker analysis (*C37*, *Cx40*, *Dll4*, *EphB2*, *Hey1*) was performed at E8.25. Embryos and YSs were individually lysed in Trizol for RNA extraction and screened for YFP positive and negative samples (n=3 each) that were stage matched at 4-7 somites (Figure S7A). Additionally, the ratio of exogenous over endogenous *mSprouty4* expression was quantitated for YFP positive samples using transcript-specific primers (Figure S7B). Detection was via the Sybr-green or Taqman assay (for arterial markers) and fold change of expression between YFP-positive and negative samples, and statistical analysis were performed as previously described.

References

ADAMS, R. H., WILKINSON, G. A., WEISS, C., DIELLA, F., GALE, N. W., DEUTSCH, U., RISAU, W. & KLEIN, R. 1999. Roles of ephrinB ligands and EphB receptors in cardiovascular development: demarcation of arterial/venous domains, vascular morphogenesis, and sprouting angiogenesis. *Genes Dev,* 13**,** 295-306.

AITSEBAOMO, J., PORTBURY, A. L., SCHISLER, J. C. & PATTERSON, C. 2008. Brothers and sisters: molecular insights into arterial-venous heterogeneity. *Circ Res,* 103**,** 929-39.

ALBERT, P. S., BROWN, S. J. & RIDDLE, D. L. 1981. Sensory control of dauer larva formation in Caenorhabditis elegans. *J Comp Neurol,* 198**,** 435-51.

BAEYENS, N. & SCHWARTZ, M. A. 2016. Biomechanics of vascular mechanosensation and remodeling. *Mol Biol Cell,* 27**,** 7-11.

BEARD, R. S., JR., HOETTELS, B. A., MEEGAN, J. E., WERTZ, T. S., CHA, B. J., YANG, X., OXFORD, J. T., WU, M. H. & YUAN, S. Y. 2020. AKT2 maintains brain endothelial claudin-5 expression and selective activation of IR/AKT2/FOXO1-signaling reverses barrier dysfunction. *J Cereb Blood Flow Metab,* 40**,** 374-391.

BERNATCHEZ, P. N., SOKER, S. & SIROIS, M. G. 1999. Vascular endothelial growth factor effect on endothelial cell proliferation, migration, and platelet-activating factor synthesis is Flk-1-dependent. *J Biol Chem,* 274**,** 31047-54.

CASCI, T., VINOS, J. & FREEMAN, M. 1999. Sprouty, an intracellular inhibitor of Ras signaling. *Cell,* 96**,** 655-65.

CHLENCH, S., MECHA DISASSA, N., HOHBERG, M., HOFFMANN, C., POHLKAMP, T., BEYER, G., BONGRAZIO, M., DA SILVA-AZEVEDO, L., BAUM, O., PRIES, A. R. & ZAKRZEWICZ, A. 2007. Regulation of Foxo-1 and the angiopoietin-2/Tie2 system by shear stress. *FEBS Lett,* 581**,** 673-80.

CHONG, D. C., KOO, Y., XU, K., FU, S. & CLEAVER, O. 2011. Stepwise arteriovenous fate acquisition during mammalian vasculogenesis. *Dev Dyn,* 240**,** 2153-65.

CHU, M., LI, T., SHEN, B., CAO, X., ZHONG, H., ZHANG, L., ZHOU, F., MA, W., JIANG, H., XIE, P., LIU, Z., DONG, N., XU, Y., ZHAO, Y., XU, G., LU, P., LUO, J., WU, Q., ALITALO, K., KOH, G. Y., ADAMS, R. H. & HE, Y. 2016. Angiopoietin receptor Tie2 is required for vein specification and maintenance via regulating COUP-TFII. *Elife,* 5.

CLEAVER, O. & KRIEG, P. A. 1998. VEGF mediates angioblast migration during development of the dorsal aorta in Xenopus. *Development,* 125**,** 3905-14.

CORADA, M., NYQVIST, D., ORSENIGO, F., CAPRINI, A., GIAMPIETRO, C., TAKETO, M. M., IRUELA-ARISPE, M. L., ADAMS, R. H. & DEJANA, E. 2010. The Wnt/beta-catenin pathway modulates vascular remodeling and specification by upregulating Dll4/Notch signaling. *Dev Cell,* 18**,** 938-49.

COVASSIN, L. D., VILLEFRANC, J. A., KACERGIS, M. C., WEINSTEIN, B. M. & LAWSON, N. D. 2006. Distinct genetic interactions between multiple Vegf receptors are required for development of different blood vessel types in zebrafish. *Proc Natl Acad Sci U S A,* 103**,** 6554-9.

DANG, L. T. H., ABURATANI, T., MARSH, G. A., JOHNSON, B. G., ALIMPERTI, S., YOON, C. J., HUANG, A., SZAK, S., NAKAGAWA, N., GOMEZ, I., REN, S., READ, S. K., SPARAGES, C., APLIN, A. C., NICOSIA, R. F., CHEN, C., LIGRESTI, G. & DUFFIELD, J. S. 2017. Hyperactive FOXO1 results in lack of tip stalk identity and deficient microvascular regeneration during kidney injury. *Biomaterials,* 141**,** 314-329.

DHARANEESWARAN, H., ABID, M. R., YUAN, L., DUPUIS, D., BEELER, D., SPOKES, K. C., JANES, L., SCIUTO, T., KANG, P. M., JAMINET, S. S., DVORAK, A., GRANT, M. A., REGAN, E. R. & AIRD, W. C. 2014. FOXO1-mediated activation of Akt plays a critical role in vascular homeostasis. *Circ Res,* 115**,** 238-251.

DICKINSON, M. E., FLENNIKEN, A. M., JI, X., TEBOUL, L., WONG, M. D., WHITE, J. K., MEEHAN, T. F., WENINGER, W. J., WESTERBERG, H., ADISSU, H., BAKER, C. N., BOWER, L., BROWN, J. M., CADDLE, L. B., CHIANI, F., CLARY, D., CLEAK, J., DALY, M. J., DENEGRE, J. M., DOE, B., DOLAN, M. E., EDIE, S. M., FUCHS, H., GAILUS-DURNER, V., GALLI, A., GAMBADORO, A., GALLEGOS, J., GUO, S., HORNER, N. R., HSU, C. W., JOHNSON, S. J., KALAGA, S., KEITH, L. C., LANOUE, L., LAWSON, T. N., LEK, M., MARK, M., MARSCHALL, S., MASON, J., MCELWEE, M. L., NEWBIGGING, S., NUTTER, L. M., PETERSON, K. A., RAMIREZ-SOLIS, R., ROWLAND, D. J., RYDER, E., SAMOCHA, K. E., SEAVITT, J. R., SELLOUM, M., SZOKE-KOVACS, Z., TAMURA, M., TRAINOR, A. G., TUDOSE, I., WAKANA, S., WARREN, J., WENDLING, O., WEST, D. B., WONG, L., YOSHIKI, A., INTERNATIONAL MOUSE PHENOTYPING, C., JACKSON, L., INFRASTRUCTURE NATIONALE PHENOMIN, I. C. D. L. S., CHARLES RIVER, L., HARWELL, M. R. C., TORONTO CENTRE FOR, P., WELLCOME TRUST SANGER, I., CENTER, R. B., MACARTHUR, D. G., TOCCHINI-VALENTINI, G. P., GAO, X.,

FLICEK, P., BRADLEY, A., SKARNES, W. C., JUSTICE, M. J., PARKINSON, H. E., MOORE, M., WELLS, S., BRAUN, R. E., SVENSON, K. L., DE ANGELIS, M. H., HERAULT, Y., MOHUN, T., MALLON, A. M., HENKELMAN, R. M., BROWN, S. D., ADAMS, D. J., LLOYD, K. C., MCKERLIE, C., BEAUDET, A. L., BUCAN, M. & MURRAY, S. A. 2016. High-throughput discovery of novel developmental phenotypes. *Nature,* 537**,** 508-514.

DIXIT, M., BESS, E., FISSLTHALER, B., HARTEL, F. V., NOLL, T., BUSSE, R. & FLEMING, I. 2008. Shear stress-induced activation of the AMP-activated protein kinase regulates FoxO1a and angiopoietin-2 in endothelial cells. *Cardiovasc Res,* 77**,** 160-8.

DUARTE, A., HIRASHIMA, M., BENEDITO, R., TRINDADE, A., DINIZ, P., BEKMAN, E., COSTA, L., HENRIQUE, D. & ROSSANT, J. 2004. Dosage-sensitive requirement for mouse Dll4 in artery development. *Genes Dev,* 18**,** 2474-8.

DYER, M. A., FARRINGTON, S. M., MOHN, D., MUNDAY, J. R. & BARON, M. H. 2001. Indian hedgehog activates hematopoiesis and vasculogenesis and can respecify prospective neurectodermal cell fate in the mouse embryo. *Development,* 128**,** 1717-30.

DZIADEK, M. & ADAMSON, E. 1978. Localization and synthesis of alphafoetoprotein in post-implantation mouse embryos. *J Embryol Exp Morphol,* 43**,** 289-313.

EKLUND, L. & OLSEN, B. R. 2006. Tie receptors and their angiopoietin ligands are context-dependent regulators of vascular remodeling. *Exp Cell Res,* 312**,** 630-41.

FANG, J. S., COON, B. G., GILLIS, N., CHEN, Z., QIU, J., CHITTENDEN, T. W., BURT, J. M., SCHWARTZ, M. A. & HIRSCHI, K. K. 2017. Shear-induced Notch-Cx37-p27 axis arrests endothelial cell cycle to enable arterial specification. *Nat Commun,* 8**,** 2149.

FERDOUS, A., MORRIS, J., ABEDIN, M. J., COLLINS, S., RICHARDSON, J. A. & HILL, J. A. 2011. Forkhead factor FoxO1 is essential for placental morphogenesis in the developing embryo. *Proc Natl Acad Sci U S A,* 108**,** 16307-12.

FISCHER, A., SCHUMACHER, N., MAIER, M., SENDTNER, M. & GESSLER, M. 2004. The Notch target genes Hey1 and Hey2 are required for embryonic vascular development. *Genes Dev,* 18**,** 901-11.

FISH, J. E., CANTU GUTIERREZ, M., DANG, L. T., KHYZHA, N., CHEN, Z., VEITCH, S., CHENG, H. S., KHOR, M., ANTOUNIANS, L., NJOCK, M. S., BOUDREAU, E., HERMAN, A. M., RHYNER, A. M., RUIZ, O. E., EISENHOFFER, G. T., MEDINA-RIVERA, A., WILSON, M. D. & WYTHE, J. D. 2017. Dynamic regulation of VEGF-inducible genes by an ERK/ERG/p300 transcriptional network. *Development,* 144**,** 2428-2444.

FISH, J. E. & WYTHE, J. D. 2015. The molecular regulation of arteriovenous specification and maintenance. *Dev Dyn,* 244**,** 391-409.

FOSBRINK, M., NICULESCU, F., RUS, V., SHIN, M. L. & RUS, H. 2006. C5b-9-induced endothelial cell proliferation and migration are dependent on Akt inactivation of forkhead transcription factor FOXO1. *J Biol Chem,* 281**,** 19009-18.

FRASER, S. T., HADJANTONAKIS, A. K., SAHR, K. E., WILLEY, S., KELLY, O. G., JONES, E. A., DICKINSON, M. E. & BARON, M. H. 2005. Using a histone yellow fluorescent protein fusion for tagging and tracking endothelial cells in ES cells and mice. *Genesis,* 42**,** 162-71.

FUKUMOTO, M., KONDO, K., UNI, K., ISHIGURO, T., HAYASHI, M., UEDA, S., MORI, I., NIIMI, K., TASHIRO, F., MIYAZAKI, S., MIYAZAKI, J. I., INAGAKI, S. & FURUYAMA, T. 2018. Tip-cell behavior is regulated by transcription factor FoxO1 under hypoxic conditions in developing mouse retinas. *Angiogenesis,* 21**,** 203-214.

FURUYAMA, T., KITAYAMA, K., SHIMODA, Y., OGAWA, M., SONE, K., YOSHIDA-ARAKI, K., HISATSUNE, H., NISHIKAWA, S., NAKAYAMA, K., NAKAYAMA, K., IKEDA, K., MOTOYAMA, N. & MORI, N. 2004. Abnormal angiogenesis in Foxo1 (Fkhr)-deficient mice. *J Biol Chem,* 279**,** 34741-9.

GALE, N. W., DOMINGUEZ, M. G., NOGUERA, I., PAN, L., HUGHES, V., VALENZUELA, D. M., MURPHY, A. J., ADAMS, N. C., LIN, H. C., HOLASH, J., THURSTON, G. & YANCOPOULOS, G. D. 2004. Haploinsufficiency of delta-like 4 ligand results in embryonic lethality due to major defects in arterial and vascular development. *Proc Natl Acad Sci U S A,* 101**,** 15949-54.

GOETZ, J. G., STEED, E., FERREIRA, R. R., ROTH, S., RAMSPACHER, C., BOSELLI, F., CHARVIN, G., LIEBLING, M., WYART, C., SCHWAB, Y. & VERMOT, J. 2014. Endothelial cilia mediate low flow sensing during zebrafish vascular development. *Cell Rep,* 6**,** 799-808.

GONG, Y., YANG, X., HE, Q., GOWER, L., PRUDOVSKY, I., VARY, C. P., BROOKS, P. C. & FRIESEL, R. E. 2013. Sprouty4 regulates endothelial cell migration via modulating integrin beta3 stability through c-Src. *Angiogenesis,* 16**,** 861-75.

GRIDLEY, T. 2010. Notch signaling in the vasculature. *Curr Top Dev Biol,* 92**,** 277-309.

HAYASHI, H. & KUME, T. 2008. Foxc transcription factors directly regulate Dll4 and Hey2 expression by interacting with the VEGF-Notch signaling pathways in endothelial cells. *PLoS One,* 3**,** e2401.

HERMAN, A. M., RHYNER, A. M., DEVINE, W. P., MARRELLI, S. P., BRUNEAU, B. G. & WYTHE, J. D. 2018. A novel reporter allele for monitoring Dll4 expression within the embryonic and adult mouse. *Biol Open,* 7.

HERZOG, Y., GUTTMANN-RAVIV, N. & NEUFELD, G. 2005. Segregation of arterial and venous markers in subpopulations of blood islands before vessel formation. *Dev Dyn,* 232**,** 1047-55.

HOSAKA, T., BIGGS, W. H., 3RD, TIEU, D., BOYER, A. D., VARKI, N. M., CAVENEE, W. K. & ARDEN, K. C. 2004. Disruption of forkhead transcription factor (FOXO) family members in mice reveals their functional diversification. *Proc Natl Acad Sci U S A,* 101**,** 2975-80.

HUANG, H. & TINDALL, D. J. 2007. Dynamic FoxO transcription factors. *J Cell Sci,* 120**,** 2479-87.

HWA, J. J., BECKOUCHE, N., HUANG, L., KRAM, Y., LINDSKOG, H. & WANG, R. A. 2017. Abnormal arterial-venous fusions and fate specification in mouse embryos lacking blood flow. *Sci Rep,* 7**,** 11965.

JI, R. P., PHOON, C. K., ARISTIZABAL, O., MCGRATH, K. E., PALIS, J. & TURNBULL, D. H. 2003. Onset of cardiac function during early mouse embryogenesis coincides with entry of primitive erythroblasts into the embryo proper. *Circ Res,* 92**,** 133-5.

JIANG, Z., TIAN, J., ZHANG, W., YAN, H., LIU, L., HUANG, Z., LOU, J. & MA, X. 2017. Forkhead Protein FoxO1 Acts as a Repressor to Inhibit Cell Differentiation in Human Fetal Pancreatic Progenitor Cells. *J Diabetes Res,* 2017**,** 6726901.

JIRAMONGKOL, Y. & LAM, E. W. 2020. FOXO transcription factor family in cancer and metastasis. *Cancer Metastasis Rev,* 39**,** 681-709.

JONES, E. A., BARON, M. H., FRASER, S. E. & DICKINSON, M. E. 2004. Measuring hemodynamic changes during mammalian development. *Am J Physiol Heart Circ Physiol,* 287**,** H1561-9.

KAPPEL, A., RONICKE, V., DAMERT, A., FLAMME, I., RISAU, W. & BREIER, G. 1999. Identification of vascular endothelial growth factor (VEGF) receptor-2 (Flk-1) promoter/enhancer sequences sufficient for angioblast and endothelial cell-specific transcription in transgenic mice. *Blood,* 93**,** 4284-92.

KIM, Y. H., CHOI, J., YANG, M. J., HONG, S. P., LEE, C. K., KUBOTA, Y., LIM, D. S. & KOH, G. Y. 2019. A MST1-FOXO1 cascade establishes endothelial tip cell polarity and facilitates sprouting angiogenesis. *Nat Commun,* 10**,** 838.

KISANUKI, Y. Y., HAMMER, R. E., MIYAZAKI, J., WILLIAMS, S. C., RICHARDSON, J. A. & YANAGISAWA, M. 2001. Tie2-Cre transgenic mice: a new model for endothelial cell-lineage analysis in vivo. *Dev Biol,* 230**,** 230-42.

KONDRYCHYN, I., KELLY, D. J., CARRETERO, N. T., NOMORI, A., KATO, K., CHONG, J., NAKAJIMA, H., OKUDA, S., MOCHIZUKI, N. & PHNG, L. K. 2020. Marcksl1 modulates endothelial cell mechanoresponse to haemodynamic forces to control blood vessel shape and size. *Nat Commun,* 11**,** 5476.

KREBS, L. T., STARLING, C., CHERVONSKY, A. V. & GRIDLEY, T. 2010. Notch1 activation in mice causes arteriovenous malformations phenocopied by ephrinB2 and EphB4 mutants. *Genesis,* 48**,** 146-50.

KREBS, L. T., XUE, Y., NORTON, C. R., SHUTTER, J. R., MAGUIRE, M., SUNDBERG, J. P., GALLAHAN, D., CLOSSON, V., KITAJEWSKI, J., CALLAHAN, R., SMITH, G. H., STARK, K. L. & GRIDLEY, T. 2000. Notch signaling is essential for vascular morphogenesis in mice. *Genes Dev,* 14**,** 1343-52.

LAKSO, M., PICHEL, J. G., GORMAN, J. R., SAUER, B., OKAMOTO, Y., LEE, E., ALT, F. W. & WESTPHAL, H. 1996. Efficient in vivo manipulation of mouse genomic sequences at the zygote stage. *Proc Natl Acad Sci U S A,* 93**,** 5860-5.

LANGLET, F., HAEUSLER, R. A., LINDEN, D., ERICSON, E., NORRIS, T., JOHANSSON, A., COOK, J. R., AIZAWA, K., WANG, L., BUETTNER, C. & ACCILI, D. 2017. Selective Inhibition of FOXO1 Activator/Repressor Balance Modulates Hepatic Glucose Handling. *Cell,* 171**,** 824-835 e18.

LAWSON, N. D., SCHEER, N., PHAM, V. N., KIM, C. H., CHITNIS, A. B., CAMPOS-ORTEGA, J. A. & WEINSTEIN, B. M. 2001. Notch signaling is required for arterial-venous differentiation during embryonic vascular development. *Development,* 128**,** 3675-83.

LAWSON, N. D., VOGEL, A. M. & WEINSTEIN, B. M. 2002. sonic hedgehog and vascular endothelial growth factor act upstream of the Notch pathway during arterial endothelial differentiation. *Dev Cell,* 3**,** 127-36.

LE NOBLE, F., FLEURY, V., PRIES, A., CORVOL, P., EICHMANN, A. & RENEMAN, R. S. 2005. Control of arterial branching morphogenesis in embryogenesis: go with the flow. *Cardiovasc Res,* 65**,** 619-28.

LE NOBLE, F., MOYON, D., PARDANAUD, L., YUAN, L., DJONOV, V., MATTHIJSEN, R., BREANT, C., FLEURY, V. & EICHMANN, A. 2004. Flow regulates arterial-venous differentiation in the chick embryo yolk sac. *Development,* 131**,** 361-75.

LEE, S. H., SCHLOSS, D. J., JARVIS, L., KRASNOW, M. A. & SWAIN, J. L. 2001. Inhibition of angiogenesis by a mouse sprouty protein. *J Biol Chem,* 276**,** 4128-33.

LIU, Z. J., SHIRAKAWA, T., LI, Y., SOMA, A., OKA, M., DOTTO, G. P., FAIRMAN, R. M., VELAZQUEZ, O. C. & HERLYN, M. 2003. Regulation of Notch1 and Dll4 by vascular endothelial growth factor in arterial endothelial cells: implications for modulating arteriogenesis and angiogenesis. *Mol Cell Biol,* 23**,** 14-25.

LOBOV, I. B., RENARD, R. A., PAPADOPOULOS, N., GALE, N. W., THURSTON, G., YANCOPOULOS, G. D. & WIEGAND, S. J. 2007. Delta-like ligand 4 (Dll4) is induced by VEGF as a negative regulator of angiogenic sprouting. *Proc Natl Acad Sci U S A,* 104**,** 3219-24.

LUCITTI, J. L., JONES, E. A., HUANG, C., CHEN, J., FRASER, S. E. & DICKINSON, M. E. 2007. Vascular remodeling of the mouse yolk sac requires hemodynamic force. *Development,* 134**,** 3317-26.

MACK, J. J. & IRUELA-ARISPE, M. L. 2018. NOTCH regulation of the endothelial cell phenotype. *Curr Opin Hematol,* 25**,** 212-218.

MACK, J. J., MOSQUEIRO, T. S., ARCHER, B. J., JONES, W. M., SUNSHINE, H., FAAS, G. C., BRIOT, A., ARAGON, R. L., SU, T., ROMAY, M. C., MCDONALD, A. I., KUO, C. H., LIZAMA, C. O., LANE, T. F., ZOVEIN, A. C., FANG, Y., TARLING, E. J., DE AGUIAR VALLIM, T. Q., NAVAB, M., FOGELMAN, A. M., BOUCHARD, L. S. & IRUELA-ARISPE, M. L. 2017. NOTCH1 is a mechanosensor in adult arteries. *Nat Commun,* 8**,** 1620.

MAILHOS, C., MODLICH, U., LEWIS, J., HARRIS, A., BICKNELL, R. & ISH-HOROWICZ, D. 2001. Delta4, an endothelial specific notch ligand expressed at sites of physiological and tumor angiogenesis. *Differentiation,* 69**,** 135-44.

MASUMURA, T., YAMAMOTO, K., SHIMIZU, N., OBI, S. & ANDO, J. 2009. Shear stress increases expression of the arterial endothelial marker ephrinB2 in murine ES cells via the VEGF-Notch signaling pathways. *Arterioscler Thromb Vasc Biol,* 29**,** 2125-31.

NIIMI, K., UEDA, M., FUKUMOTO, M., KOHARA, M., SAWANO, T., TSUCHIHASHI, R., SHIBATA, S., INAGAKI, S. & FURUYAMA, T. 2017. Transcription factor FOXO1 promotes cell migration toward exogenous ATP via controlling P2Y1 receptor expression in lymphatic endothelial cells. *Biochem Biophys Res Commun,* 489**,** 413-419.

OBI, S., YAMAMOTO, K., SHIMIZU, N., KUMAGAYA, S., MASUMURA, T., SOKABE, T., ASAHARA, T. & ANDO, J. 2009. Fluid shear stress induces arterial differentiation of endothelial progenitor cells. *J Appl Physiol (1985),* 106**,** 203-11.

PAIK, J. H., KOLLIPARA, R., CHU, G., JI, H., XIAO, Y., DING, Z., MIAO, L., TOTHOVA, Z., HORNER, J. W., CARRASCO, D. R., JIANG, S., GILLILAND, D. G., CHIN, L., WONG, W. H., CASTRILLON, D. H. & DEPINHO, R. A. 2007. FoxOs are lineage-restricted redundant tumor suppressors and regulate endothelial cell homeostasis. *Cell,* 128**,** 309-23.

PALIS, J. 2014. Primitive and definitive erythropoiesis in mammals. *Front Physiol,* 5**,** 3.

PFAFFL, M. W. 2001. A new mathematical model for relative quantification in real-time RT-PCR. *Nucleic Acids Res,* 29**,** e45.

POTENTE, M., URBICH, C., SASAKI, K., HOFMANN, W. K., HEESCHEN, C., AICHER, A., KOLLIPARA, R., DEPINHO, R. A., ZEIHER, A. M. & DIMMELER, S. 2005. Involvement of Foxo transcription factors in angiogenesis and postnatal neovascularization. *J Clin Invest,* 115**,** 2382-92.

RIDDELL, M., NAKAYAMA, A., HIKITA, T., MIRZAPOURSHAFIYI, F., KAWAMURA, T., PASHA, A., LI, M., MASUZAWA, M., LOOSO, M., STEINBACHER, T., EBNET, K., POTENTE, M., HIROSE, T., OHNO, S., FLEMING, I., GATTENLOHNER, S., AUNG, P. P., PHUNG, T., YAMASAKI, O., YANAGI, T., UMEMURA, H. & NAKAYAMA, M. 2018. aPKC controls endothelial growth by modulating c-Myc via FoxO1 DNA-binding ability. *Nat Commun,* 9**,** 5357.

RISAU, W. 1994. Angiogenesis and endothelial cell function. *Arzneimittelforschung,* 44**,** 416-7.

RISAU, W. & FLAMME, I. 1995. Vasculogenesis. *Annu Rev Cell Dev Biol,* 11**,** 73-91.

RONICKE, V., RISAU, W. & BREIER, G. 1996. Characterization of the endothelium-specific murine vascular endothelial growth factor receptor-2 (Flk-1) promoter. *Circ Res,* 79**,** 277-85.

RUDNICKI, M., ABDIFARKOSH, G., NWADOZI, E., RAMOS, S. V., MAKKI, A., SEPA-KISHI, D. M., CEDDIA, R. B., PERRY, C. G., ROUDIER, E. & HAAS, T. L. 2018. Endothelial-specific FoxO1 depletion prevents obesity-related disorders by increasing vascular metabolism and growth. *Elife,* 7.

SACILOTTO, N., MONTEIRO, R., FRITZSCHE, M., BECKER, P. W., SANCHEZ-DEL-CAMPO, L., LIU, K., PINHEIRO, P., RATNAYAKA, I., DAVIES, B., GODING, C. R., PATIENT, R., BOU-GHARIOS, G. & DE VAL, S. 2013. Analysis of Dll4 regulation reveals a combinatorial role for Sox and Notch in arterial development. *Proc Natl Acad Sci U S A,* 110**,** 11893-8.

SCHLAEGER, T. M., BARTUNKOVA, S., LAWITTS, J. A., TEICHMANN, G., RISAU, W., DEUTSCH, U. & SATO, T. N. 1997. Uniform vascular-endothelial-cell-specific gene expression in both embryonic and adult transgenic mice. *Proc Natl Acad Sci U S A,* 94**,** 3058-63.

SENGUPTA, A., CHAKRABORTY, S., PAIK, J., YUTZEY, K. E. & EVANS-ANDERSON, H. J. 2012. FoxO1 is required in endothelial but not myocardial cell lineages during cardiovascular development. *Dev Dyn,* 241**,** 803-13.

SEO, S., FUJITA, H., NAKANO, A., KANG, M., DUARTE, A. & KUME, T. 2006. The forkhead transcription factors, Foxc1 and Foxc2, are required for arterial specification and lymphatic sprouting during vascular development. *Dev Biol,* 294**,** 458-70.

SHAY-SALIT, A., SHUSHY, M., WOLFOVITZ, E., YAHAV, H., BREVIARIO, F., DEJANA, E. & RESNICK, N. 2002. VEGF receptor 2 and the adherens junction as a mechanical transducer in vascular endothelial cells. *Proc Natl Acad Sci U S A,* 99**,** 9462-7.

SHUTTER, J. R., SCULLY, S., FAN, W., RICHARDS, W. G., KITAJEWSKI, J., DEBLANDRE, G. A., KINTNER, C. R. & STARK, K. L. 2000. Dll4, a novel Notch ligand expressed in arterial endothelium. *Genes Dev,* 14**,** 1313-8.

SIEKMANN, A. F. & LAWSON, N. D. 2007. Notch signalling limits angiogenic cell behaviour in developing zebrafish arteries. *Nature,* 445**,** 781-4.

SU, T., STANLEY, G., SINHA, R., D'AMATO, G., DAS, S., RHEE, S., CHANG, A. H., PODURI, A., RAFTREY, B., DINH, T. T., ROPER, W. A., LI, G., QUINN, K. E., CARON, K. M., WU, S., MIQUEROL, L., BUTCHER, E. C., WEISSMAN, I., QUAKE, S. & RED-HORSE, K. 2018. Single-cell analysis of early progenitor cells that build coronary arteries. *Nature,* 559**,** 356-362.

SUN, X., CHEN, W. D. & WANG, Y. D. 2017. DAF-16/FOXO Transcription Factor in Aging and Longevity. *Front Pharmacol,* 8**,** 548.

SWIFT, M. R. & WEINSTEIN, B. M. 2009. Arterial-venous specification during development. *Circ Res,* 104**,** 576-88.

TANIGUCHI, K., ISHIZAKI, T., AYADA, T., SUGIYAMA, Y., WAKABAYASHI, Y., SEKIYA, T., NAKAGAWA, R. & YOSHIMURA, A. 2009. Sprouty4 deficiency potentiates Ras-independent angiogenic signals and tumor growth. *Cancer Sci,* 100**,** 1648-54.

TZIMA, E., IRANI-TEHRANI, M., KIOSSES, W. B., DEJANA, E., SCHULTZ, D. A., ENGELHARDT, B., CAO, G., DELISSER, H. & SCHWARTZ, M. A. 2005. A mechanosensory complex that mediates the endothelial cell response to fluid shear stress. *Nature,* 437**,** 426-31.

UDAN, R. S., VADAKKAN, T. J. & DICKINSON, M. E. 2013. Dynamic responses of endothelial cells to changes in blood flow during vascular remodeling of the mouse yolk sac. *Development,* 140**,** 4041-50.

WANG, H. U., CHEN, Z. F. & ANDERSON, D. J. 1998. Molecular distinction and angiogenic interaction between embryonic arteries and veins revealed by ephrin-B2 and its receptor Eph-B4. *Cell,* 93**,** 741-53.

WEINSTEIN, B. M. & LAWSON, N. D. 2002. Arteries, veins, Notch, and VEGF. *Cold Spring Harb Symp Quant Biol,* 67**,** 155-62.

WIETECHA, M. S., CHEN, L., RANZER, M. J., ANDERSON, K., YING, C., PATEL, T. B. & DIPIETRO, L. A. 2011. Sprouty2 downregulates angiogenesis during mouse skin wound healing. *Am J Physiol Heart Circ Physiol,* 300**,** H459-67.

WILHELM, K., HAPPEL, K., EELEN, G., SCHOORS, S., OELLERICH, M. F., LIM, R., ZIMMERMANN, B., ASPALTER, I. M., FRANCO, C. A., BOETTGER, T., BRAUN, T., FRUTTIGER, M., RAJEWSKY, K., KELLER, C., BRUNING, J. C., GERHARDT, H., CARMELIET, P. & POTENTE, M. 2016. FOXO1 couples metabolic activity and growth state in the vascular endothelium. *Nature,* 529**,** 216-20.

WRAGG, J. W., DURANT, S., MCGETTRICK, H. M., SAMPLE, K. M., EGGINTON, S. & BICKNELL, R. 2014. Shear stress regulated gene expression and angiogenesis in vascular endothelium. *Microcirculation,* 21**,** 290-300.

WYTHE, J. D., DANG, L. T., DEVINE, W. P., BOUDREAU, E., ARTAP, S. T., HE, D., SCHACHTERLE, W., STAINIER, D. Y., OETTGEN, P., BLACK, B. L., BRUNEAU, B. G. & FISH, J. E. 2013. ETS factors regulate Vegf-dependent arterial specification. *Dev Cell,* 26**,** 45-58.

XUE, Y., GAO, X., LINDSELL, C. E., NORTON, C. R., CHANG, B., HICKS, C., GENDRON-MAGUIRE, M., RAND, E. B., WEINMASTER, G. & GRIDLEY, T. 1999. Embryonic lethality and vascular defects in mice lacking the Notch ligand Jagged1. *Hum Mol Genet,* 8**,** 723-30.

YOU, L. R., LIN, F. J., LEE, C. T., DEMAYO, F. J., TSAI, M. J. & TSAI, S. Y. 2005. Suppression of Notch signalling by the COUP-TFII transcription factor regulates vein identity. *Nature,* 435**,** 98-104.

ZHANG, H., GE, S., HE, K., ZHAO, X., WU, Y., SHAO, Y. & WU, X. 2019. FoxO1 inhibits autophagosome-lysosome fusion leading to endothelial autophagic-apoptosis in diabetes. *Cardiovasc Res,* 115**,** 2008-2020.

ZHAO, Y., YANG, J., LIAO, W., LIU, X., ZHANG, H., WANG, S., WANG, D., FENG, J., YU, L. & ZHU, W. G. 2010. Cytosolic FoxO1 is essential for the induction of autophagy and tumour suppressor activity. *Nat Cell Biol,* 12**,** 665-75.

Figures

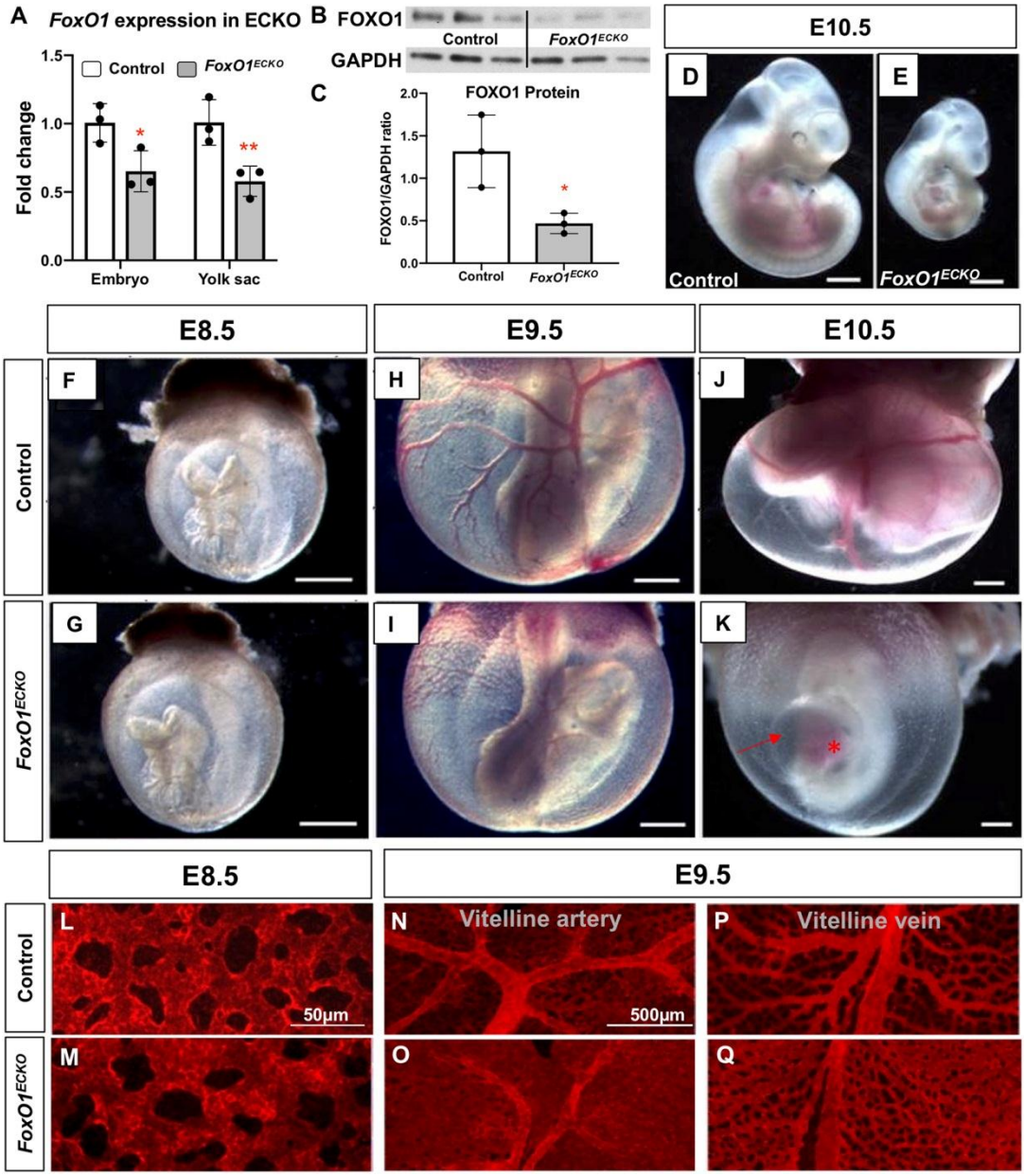

Figure 1. *FoxO1*^{ECKO} results in vascular remodeling defects and lethality. (A) qRT-PCR for *FoxO1* expression in E8.5 control and ECKO YSs. *P*<0.01. (B and C) FOXO1 protein expression in E8.5 control and ECKO YS (n=3) by western and quantification. (D and E) Bright field images of E10.5 littermate control and *FoxO1*^{ECKO} embryos. Control and *FoxO1*^{ECKO}

embryos within the YS at E8.5 (F and G), E9.5 (H and I), and E10.5 (J and K). Scale bar = 500μm. (K) Pericardial edema (arrow), blood pooling in the heart (asterisk). (L-Q) Pecam1 staining in E8.25 and 9.5 control and CKO YSs. Bars in graphs are means ± standard deviation.

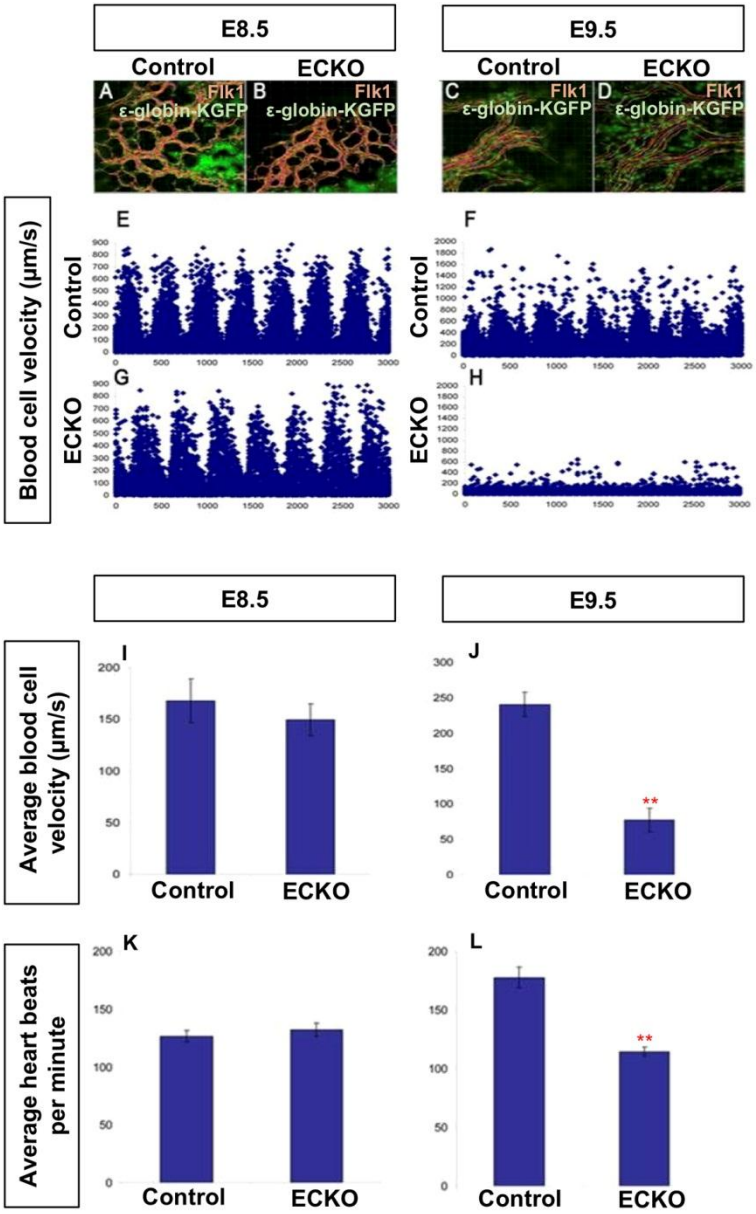

Figure 2. Vascular remodeling defects in *FoxO1*^{ECKO} embryos do not result from reduced blood flow. Primitive erythroblasts in circulation in wild type and CKO embryos were marked by crossing to an *ε-globin-GFP* transgenic reporter. Representative still images of E8.5 wild type (A), ECKO (B), E9.5 wild type (C), and ECKO (D) embryos. Individual blood cells from A-D

were tracked and velocity profiles are plotted in E-H. Quantification of the average blood velocity are graphed in I and J (Mann-Whitney U test, p=0.005). Average heart rates quantified in wild type and ECKO embryos at E8.5 (K) and E9.5 (L) (Kruskal-Wallis test, p=0.003). Bars in graphs are means ± standard error.

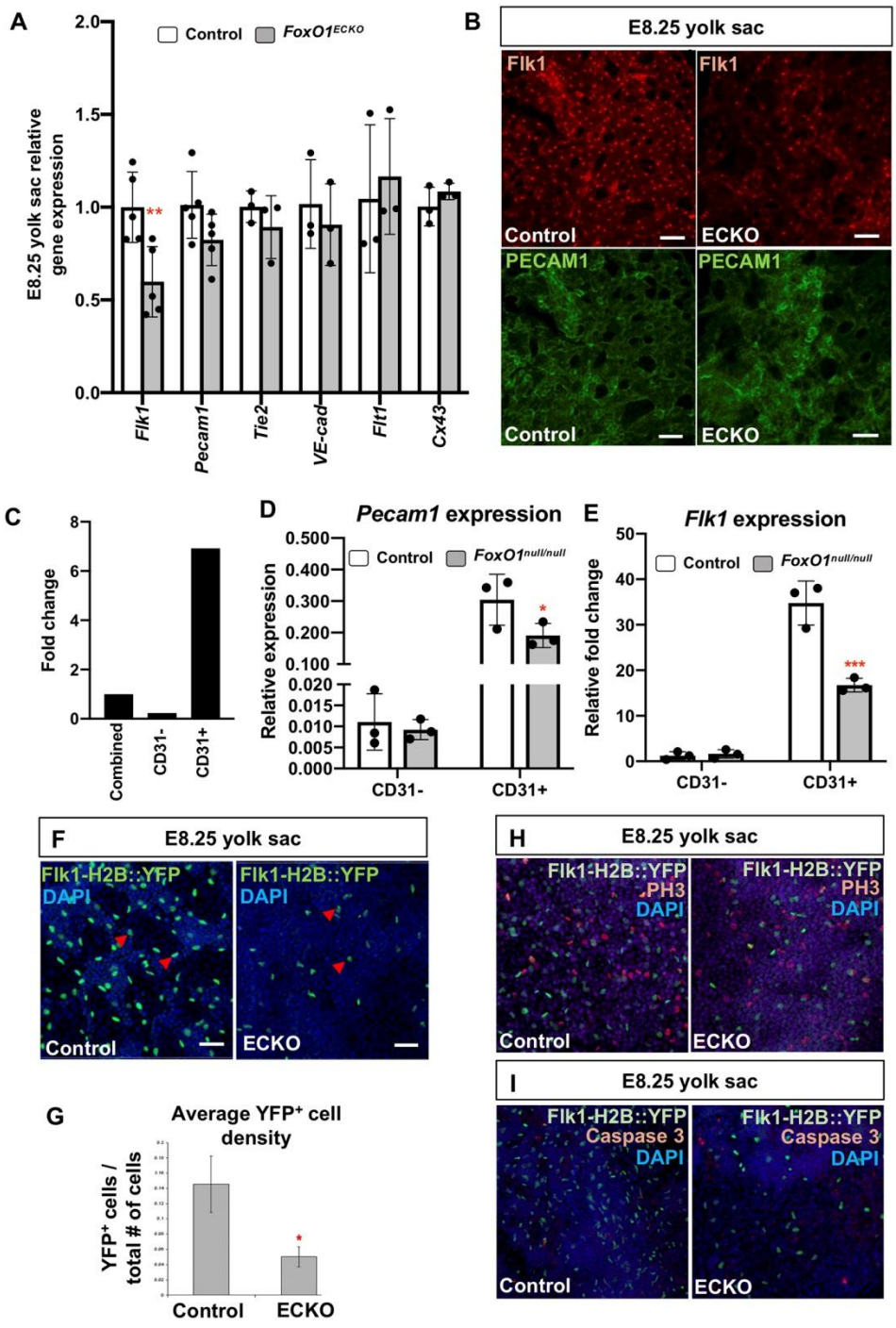

Figure 3. FOXO1 regulates FLK1 expression without affecting other endothelial genes or EC viability prior to blood flow. (A) Expression levels of endothelial genes by quantitative RT-PCR. (B) Immuno-labeling for endogenous Flk1 and Pecam1 in control and *FoxO1*^{ECKO} YSs.

Scale bars = 50μm. (C) Comparison of *Pecam1* expression in MACS sorted CD31-, CD31+, and combined control E8.25 YS cells by qPCR. Relative *Pecam1* (D) and *Flk1* (E) expression between WT and *FoxO1*^{null} E8.25 MACS sorted CD31- and CD31+ YS cells. (F) YSs from control and *FoxO1*^{ECKO} at E8.25 DAPI-stained and positive for *Flk1-H2B::YFP* transgene, which marks the EC nuclei (arrowheads). (G) Graph shows quantification of YFP+ cells relative to total number of cells labeled by DAPI from panel F. Whole mount phosphoHistone-H3 (PH3) (H) or activated Caspase3 (I) staining of control and *FoxO1*^{ECKO} E8.25 YSs co-labeled with *Flk1-H2B::YFP* transgene and DAPI. Bars in graphs are means ± standard deviation. n=3.

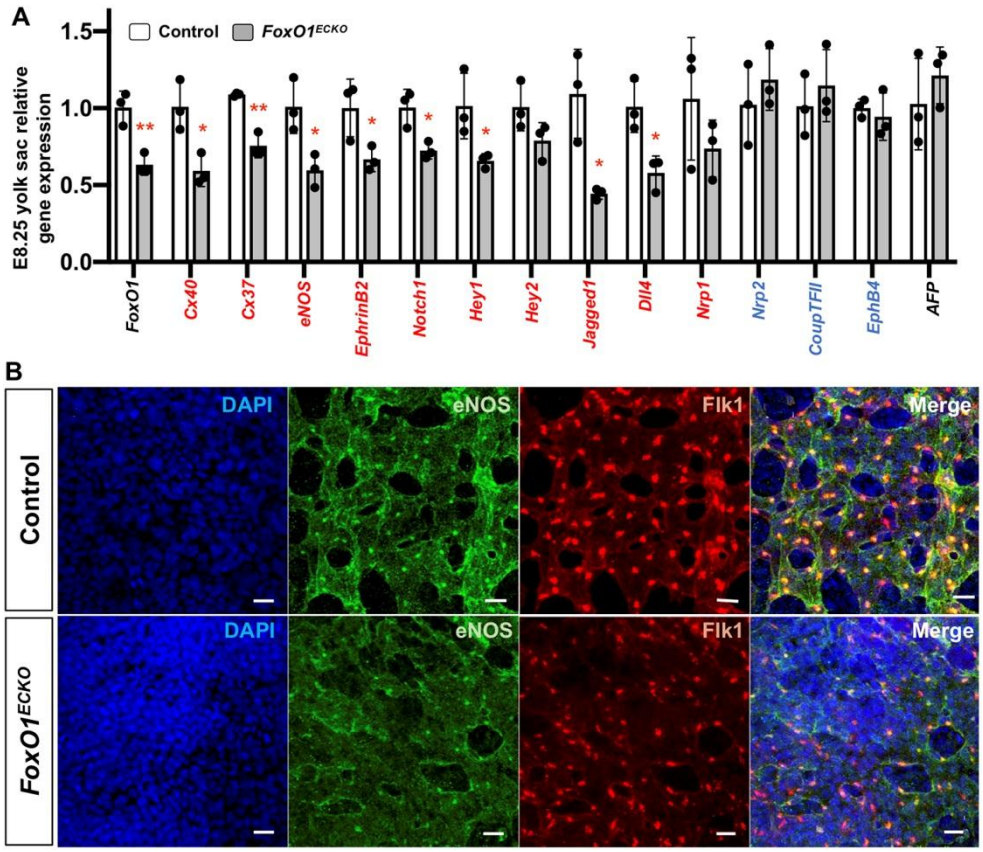

Figure 4. Arterial marker expression is reduced in *FoxO1*^{ECKO} YS. (A) **q**RT-PCR expression analysis in control and *FoxO1*^{ECKO} YSs; arterial (red), venous (blue), and endoderm markers at E8.25. **p*<0.05, ***p*<0.01, data are means ± standard deviation n=3. (B) Co-immuno labeling of eNOS, FLK1, and DAPI in control and *FoxO1*^{ECKO} YSs at E8.25. Scale bars = 20μm.

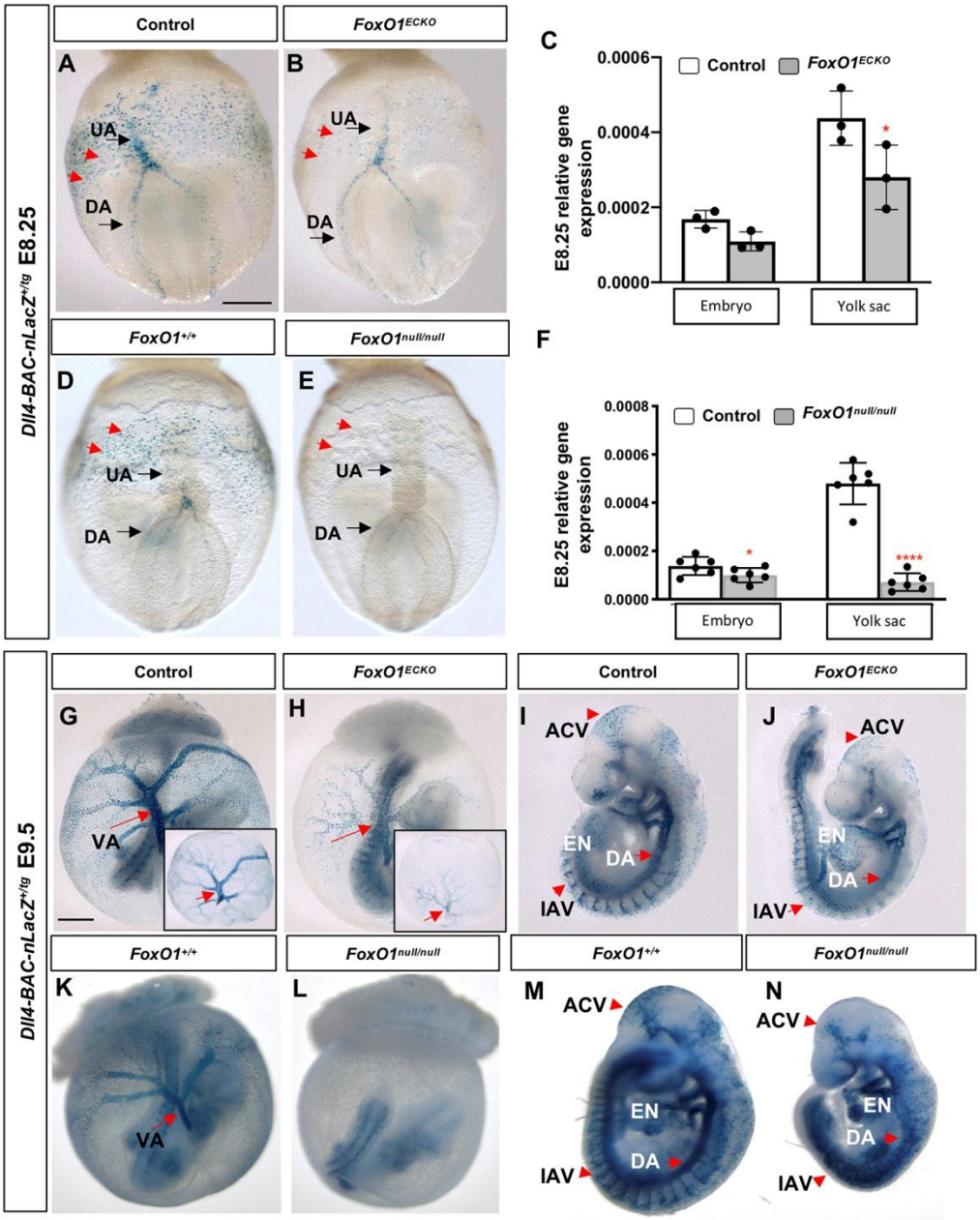

Figure 5. Characterization of arterial defects in *FoxO1*^{ECKO} and germline mutants using the *Dll4-BAC-nlacZ* reporter (A and B, D and E) *nlacZ* reporter activity was detected in the dorsal aorta [DA] and umbilical artery [UA] in E8.25 littermate control, *FoxO1*^{ECKO}, and *FoxO1* null embryos. Arrowheads point to YS ECs in posterior region of YS plexus. (C and F) qRT-PCR for *Dll4* mRNA expression in littermate control, *FoxO1*^{ECKO}, and *FoxO1* null embryos and YSs.

n>3. *p<0.05. (G and H, K and L) *nlacZ* reporter activity in E9.5 littermate control, *FoxO1*^{ECKO}, and *FoxO1* null YS and embryo; VA = vitelline artery [arrow]; insets in G and H show YSs only. (I and J, M and N) *nlacZ* reporter activity in E9.5 littermate control, *FoxO1*^{ECKO}, and *FoxO1* null; EN = endocardium, DA = dorsal aorta, IAV = intersomitic arterial vessels, ACV = arterial cranial vasculature. Scale bars for E8.25 panes = 200μm; E9.25 = 500μm. Bars in graphs are means ± standard deviation.

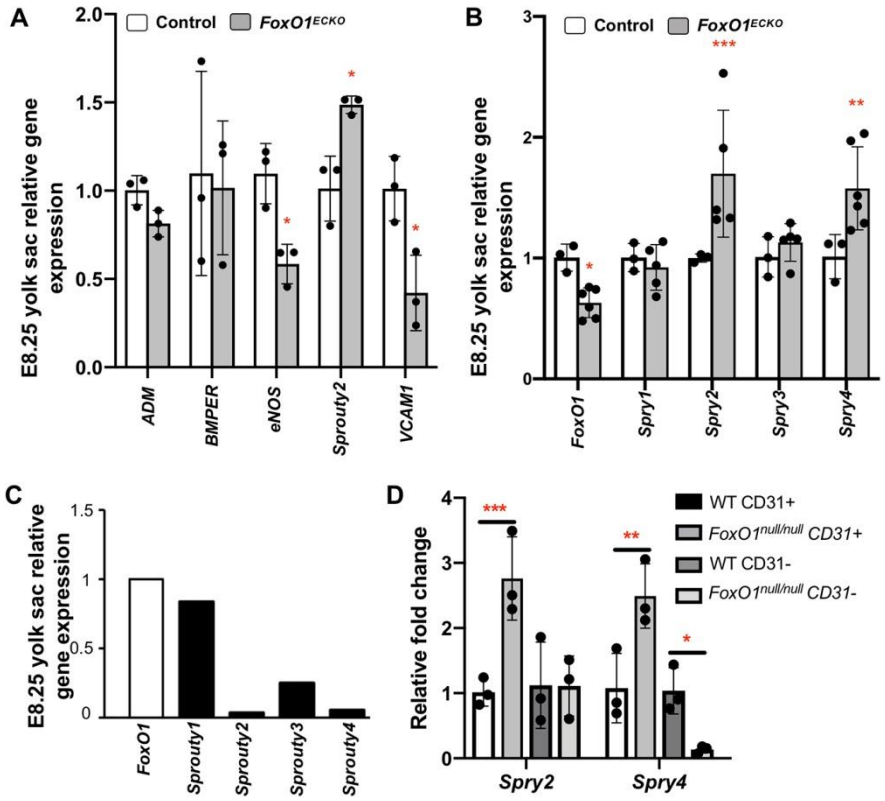

Figure 6. FOXO1 regulates *Sprouty2/4* expression in the YS vasculature. qRT-PCR analysis in littermate E8.25 control and *FoxO1*^{ECKO} YSs for (A) known FOXO1 targets and (B) *Sprouty* family members. (C) q RT-PCR of endogenous *Sprouty1-4* expression relative to *FoxO1*. (D) Quantitative RT-PCR of *Sprouty2/4* in MACS sorted E8.25 CD31+ and CD31- control and *FoxO1*^{null} YS cells. Bars in graphs are means ± standard deviation. n=3.

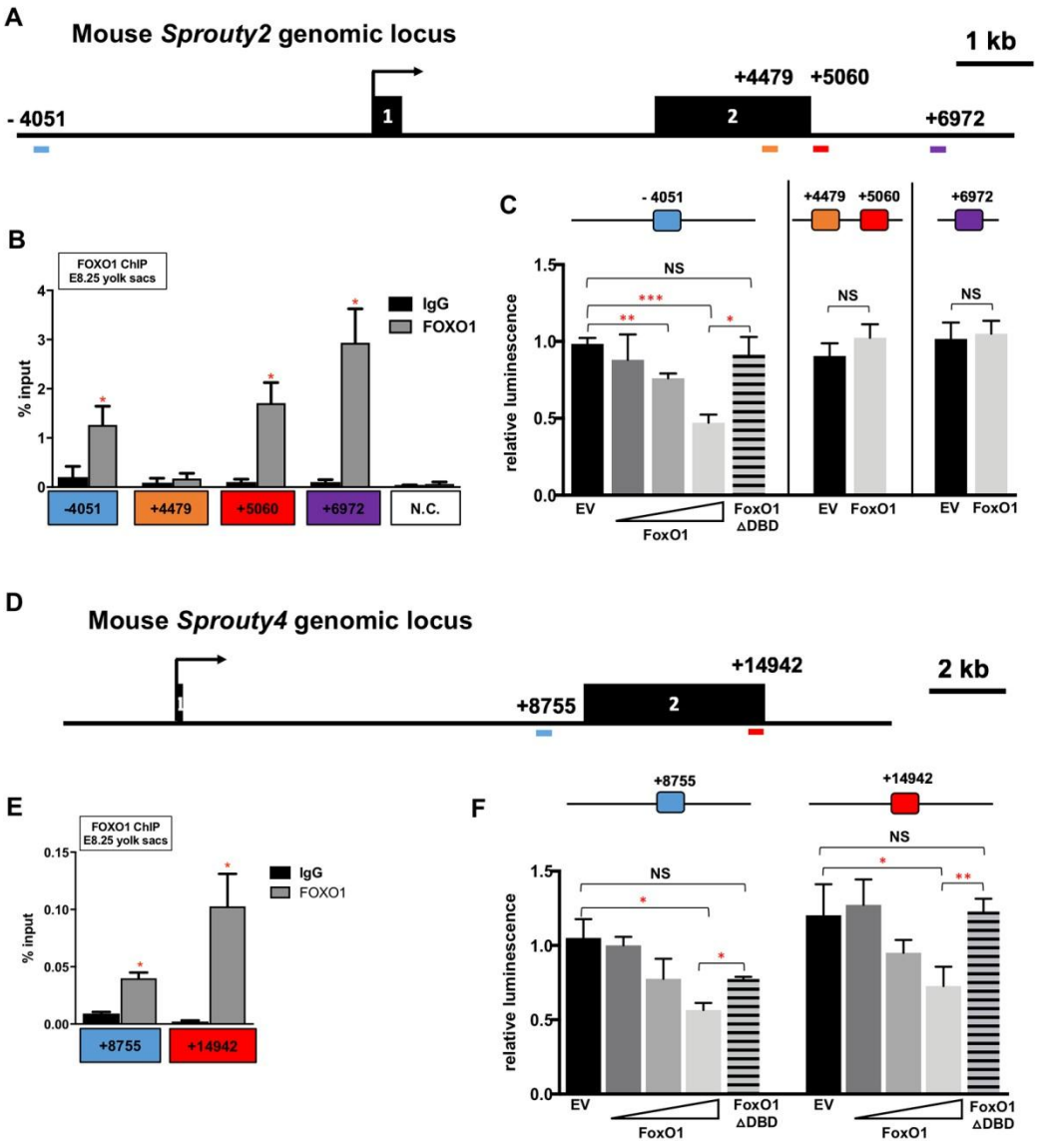

Figure 7. FOXO1 directly binds to endogenous *Sprouty2/4* promoters and represses *Sprouty2/4* transcription. (A) Genomic locus of mouse *Sprouty2* gene with FOXO1 binding sites in red. (B and E) FOXO1 ChIP-PCR using E8.25 YS chromatin. (C) Luciferase activity of FOXO1 on *Sprouty2* promoter in H1299 cells. (D) Genomic locus of mouse *Sprouty4* gene with FOXO1 binding sites in red. (F) Luciferase activity of FOXO1 on *Sprouty4* promoter in H1299 cells. **p*<0.05, ***p*<0.01, ****p*<0.001. EV, empty vector.

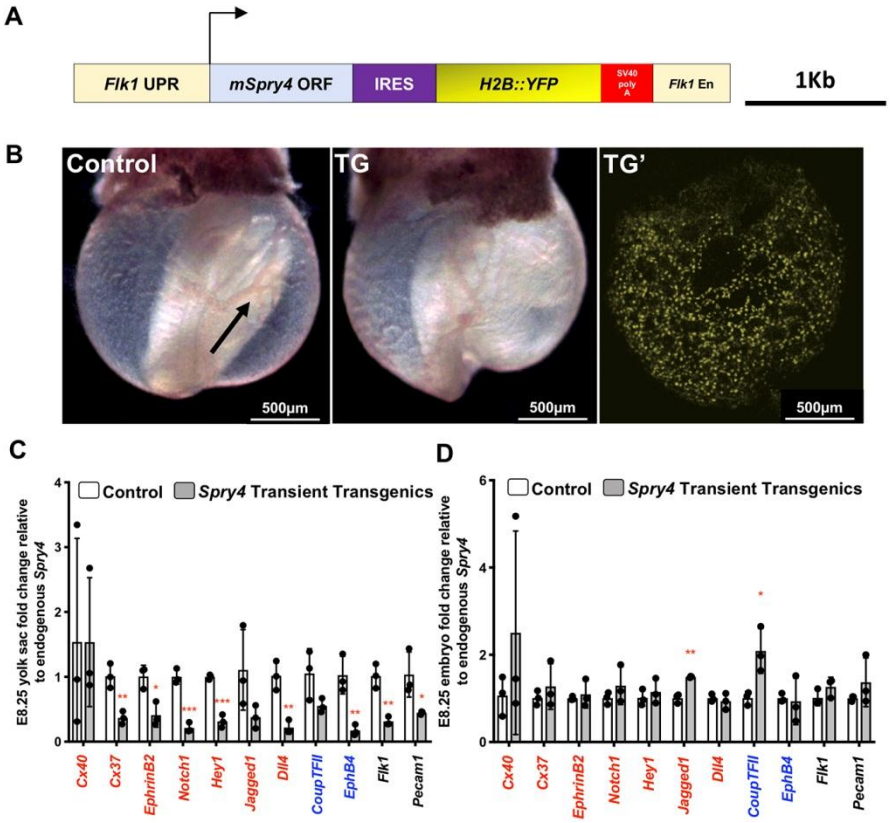

Figure 8. Transient overexpression of *Sprouty4* in ECs partially phenocopies *FoxO1*^{ECKO} mutants. (A) Schematic of *Sprouty4* overexpression construct for pro-nuclei injection. (B) Brightfield image of E9.5 non-transgenic (control) and transgenic embryo (TG); confocal imaging of TG embryo showing YFP fluorescence in YS. Note vessel remodeling in the control YS (arrow). qRT-PCR of arterial markers in E8.25 control and TG YSs (C) and embryos (D) (n=3). *p<0.05, **p<0.01, ***p<0.001. Bars in graph are means ± standard deviation.

Table 1. Allantois phenotype analysis in control, null and ECKO embryos at E9.5.

Table 1	Genotype	Number of Embryos	Percent of Total	# With Gross Allantois Defects	Percent of Genotype
Germline 4 Litters	WT	16	31.37%		
	FoxO1$^{+/null}$	20	39.22%		
	FoxO1$^{null/null}$	15	29.41%	2	13.33%
	Total	51			
Conditional 6 Litters	*FoxO1*$^{+/flox}$	15	31.91%		
	FoxO1$^{+/flox}$*;Tie2-cre*$^{+/Tg}$	12	25.53%		
	FoxO1$^{flox/flox}$	10	21.28%		
	FoxO1$^{flox/flox}$*;Tie2-cre*$^{+/Tg}$	10	21.28%	0	
	Total	47			

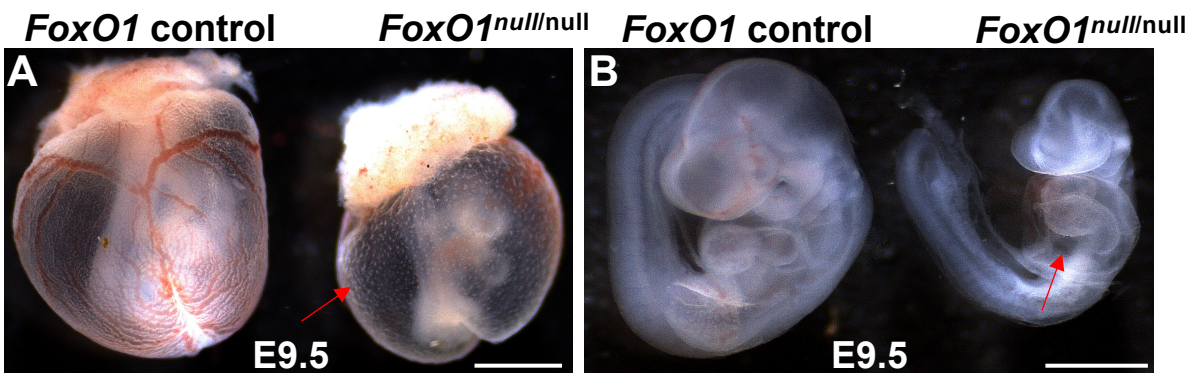

Fig. S1. *FoxO1*^{null} embryos show vascular remodeling defects. (A and B) Bright field images of E9.5 littermate control and *FoxO1*^{null} embryos in and out of the YS. (C) qRT-PCR for FoxO1 expression in control and *FoxO1*^{null} YSs.

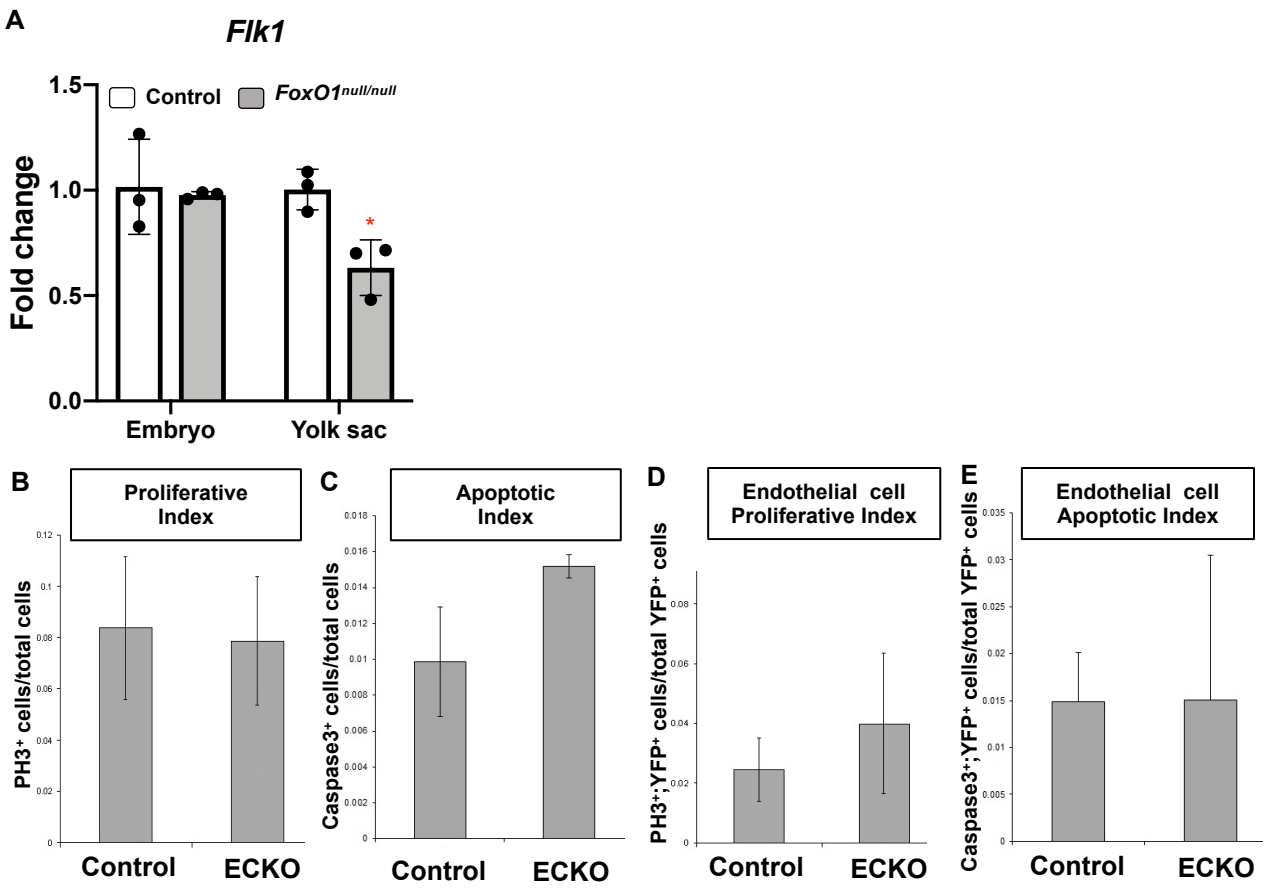

Fig. S2. (A) Flk1 expression in littermate control and *FoxO1*^{null} embryos and YSs by qRT-PCR. (B and C) Quantification of proliferation and apoptosis in littermate control and *FoxO1*^{ECKO} YSs. (D and E) Quantification of proliferation and apoptosis in littermate control and *FoxO1*^{ECKO} YS YFP+ ECs.

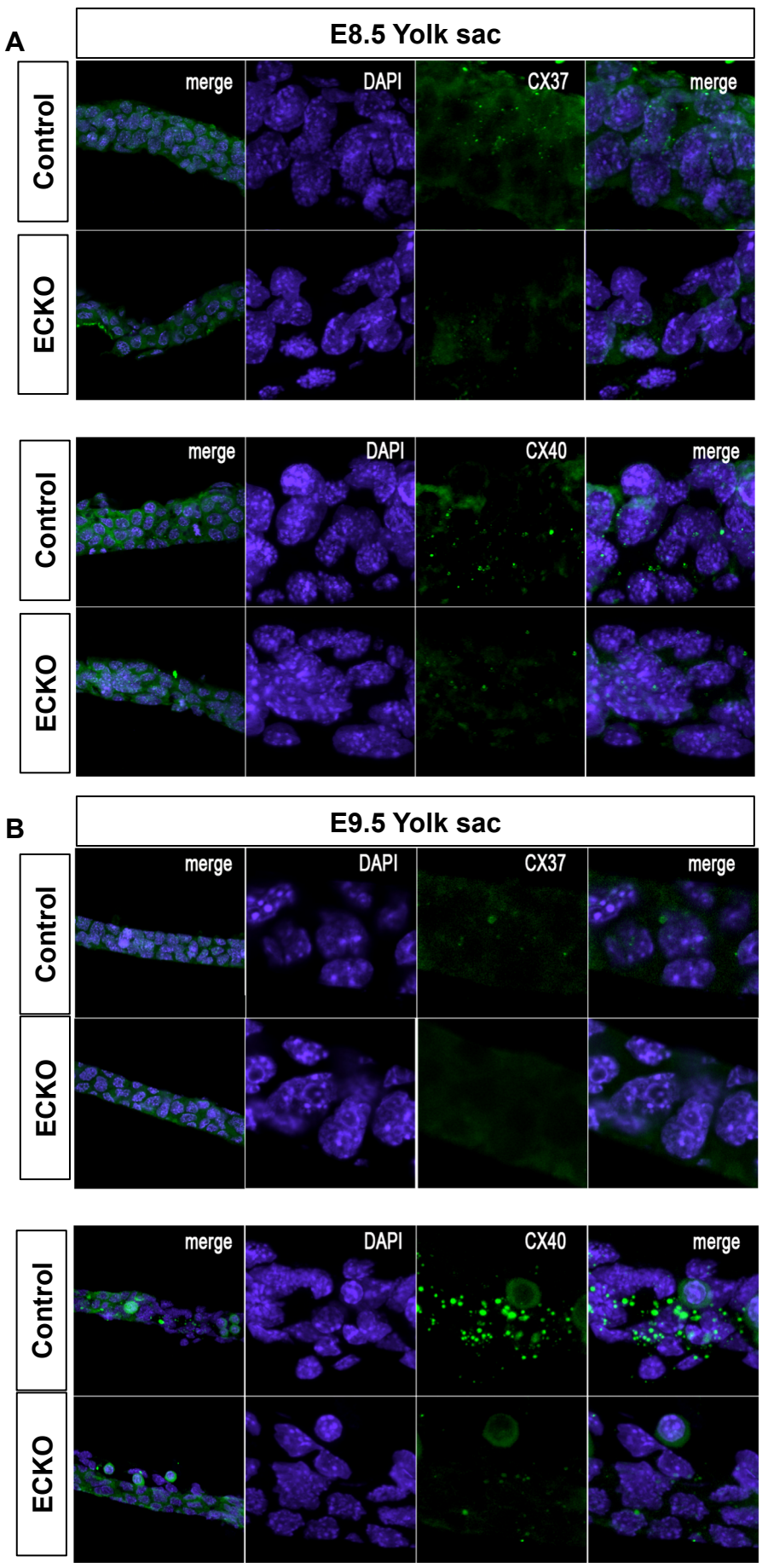

• **Fig. S3.** Co-immuno labeling of CX37, CX40and DAPI in control and *FoxO1*^{ECKO} YSs at E8.25 (A) and E9.5 (B).

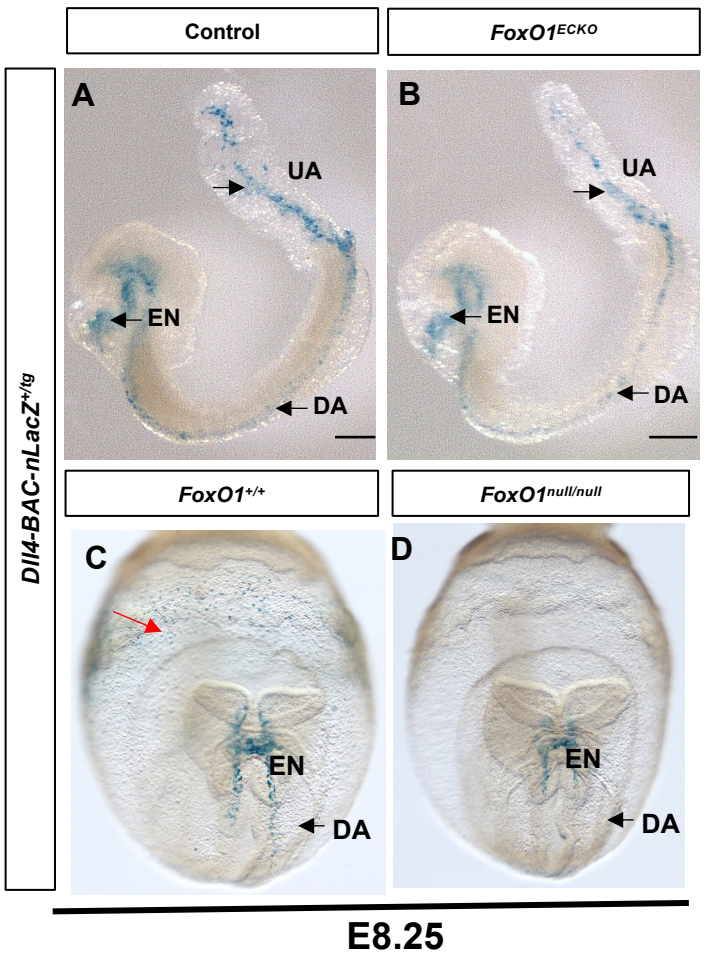

• **Fig. S4.** (A and B) *nlacZ* reporter activity in E8.25 littermate control and *FoxO1*^{ECKO} embryos dissected out of the yolk sac. (C and D) Anterior views of *nlacZ* reporter activity in E8.25 littermate control and *FoxO1*^{null} embryos. UA = umbilical artery, EN = endocardium, DA = dorsal aorta.

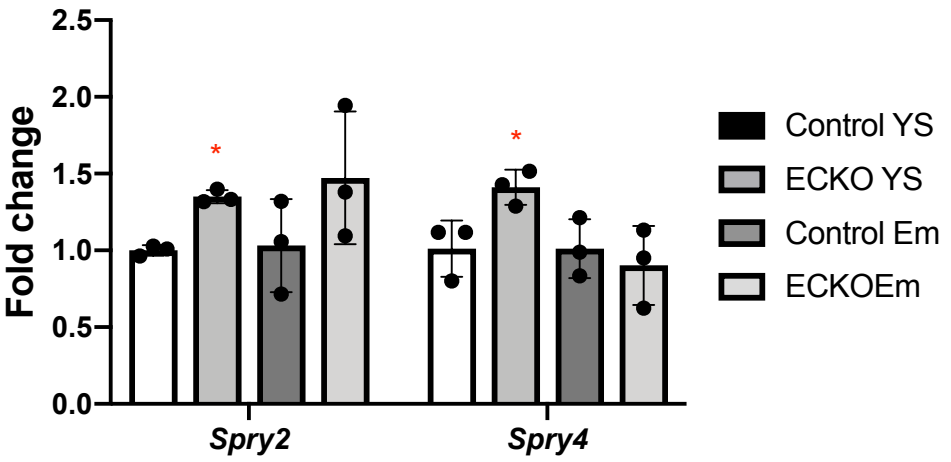

• **Fig. S5.** qRT-PCR for Sprouty2/4 in littermate control and *FoxO1*^{ECKO} YSs and embryos. Bars in graph are means± standard deviation.

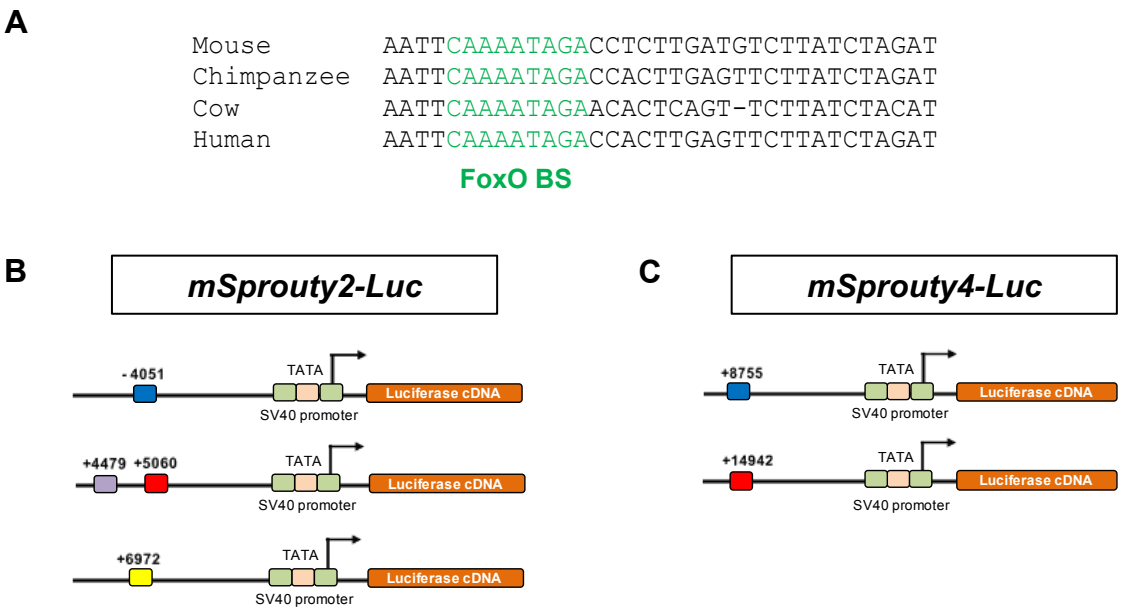

- **Fig. S6.** (A) FOXO1 conserved binding site in Mouse, Chimpanzee, Cow, and Human. (B and C) Luciferase constructs containing FOXO1 binding sites for *Sprouty2* and *Sprouty4*.

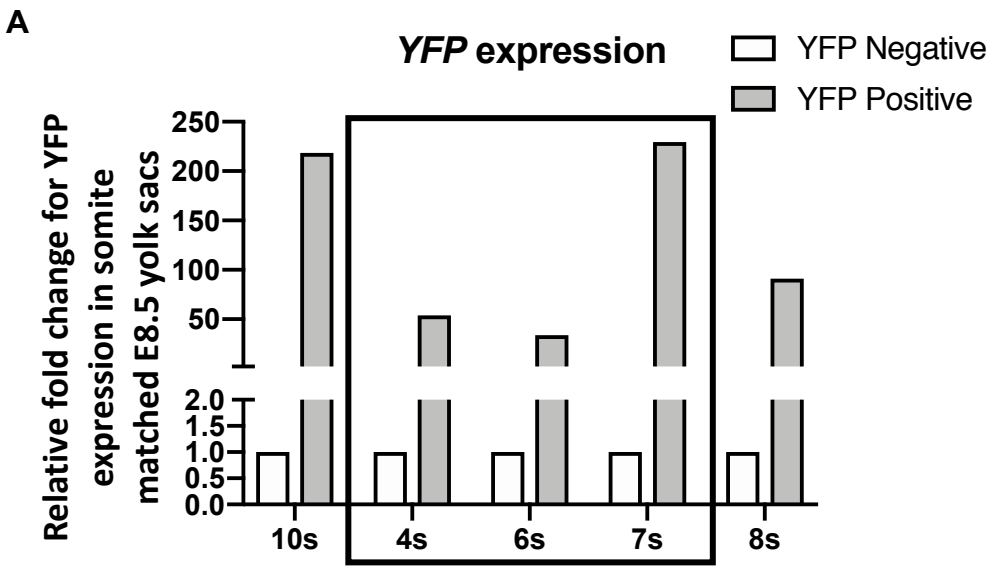

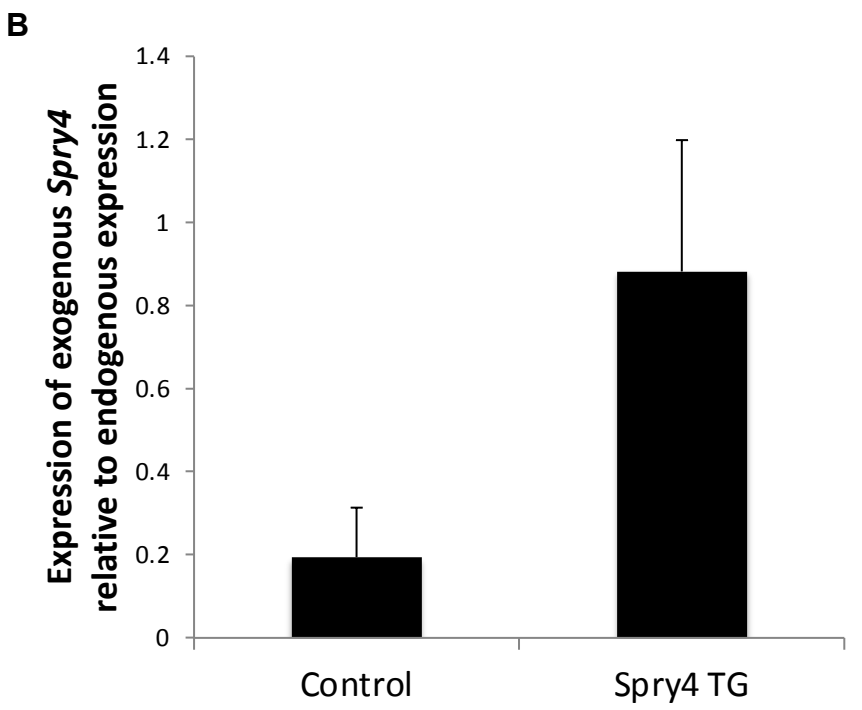

- **Fig. S7.** (A) qRT-PCR for *YFP* expression in somite matched non-trangenic (control) and transgenic embryos. Black box indicates samples that fall withing E8.25 somite stage and used for further gene analysis.
  (B) qRT-PCR for relative expression of exogenous *Sprouty4* to endogenous *Sprouty4* for all *YFP*+ transgenic embryos and somite matched controls. Bars in graph are means ± standard deviation.

Table S1. Primer sequences used for genotyping, ChIP-qPCR, and cloning

Gene/allele		Primer sequences (5'-3')	Purpose
ChIP *mSprouty2*	(-4051)	TTCCAGTCCTCCAAGCAATCTAG AGTGCCTCCAGGAAGGGAAT	ChIP-qPCR
ChIP *mSprouty2*	(4479)	AATTAGCAAATGGCTCCCGG TTTGTGACTGTGCCATGAAGC	ChIP-qPCR
ChIP *mSprouty2*	(5060)	TAGGGCGACTCAGTGGCTATC GACCGGAGTCAAAGGACCTTC	ChIP-qPCR
ChIP *mSprouty2*	(6972)	CATTTGTGTGTTTTGGGGAGAGAT CGGCAGTTGGGTTGGAATTA	ChIP-qPCR
ChIP *mSprouty4*	(8755)	GATCTCCATCCGAATTCCAAATG CTTGGTTCGGCAAAGGCGAGAAAC	ChIP-qPCR
ChIP *mSprouty4*	(14942)	CCACCACAAAAGTTACCACAGAAG GATATCTTCTAGATCAGTAC	ChIP-qPCR
ChIP negative control		GAAACCCGAATCTACATTCCGTTCC CTGGATTAACCCGATTATACACC	ChIP-qPCR
Luc *mSprouty2*	(-4051)	GTGTACACAGGTATACTCTAGTCACCAACCC GGGACTCGATGTTGCAATGAGATACTCAACTC	PCR cloning
Luc m *Sprouty2*	(4479/5060)	GATCTGTGACAAGCAGTGCCTCTGCTCAG GCCACAAGGTGACTAATGTTGTCAAGATGG	PCR cloning
Luc *mSprouty2*	(6972)	CATTCAGACCTAGCACTGTGATTCATGC CAGTGTTCAGCCAAACCAGGTAGGCCTTGA	PCR cloning
Luc *mSprouty4*	(8755)	CAGCGGTTCACTTGAAGCTGCCTTGACAAG CTCTGCCTCCCAACTGCTGGGATTAAAG	PCR cloning
Luc *mSprouty4*	(14942)	CTGTAGCTGTTTCTGACTTCTTGGCTAGC GGCTGAAGACTCATTGTAGAATGGGTCATG	PCR cloning
Endogenous	*mSpry4 cDNA*	GAAGCCTGTCCCTTGGTGCAGTTCAG CTGGTCAATGGGTAAGATGGTGAGTG	qRT-PCR
Exogenous	*mSpry4 cDNA*	GCGAGGTGCAGGAATTCGTTAAGCTCTCCC CTGGTCAATGGGTAAGATGGTGAGTG	qRT-PCR

* pGL3-Promoter

Table S2. Taqman assays for Gene expression analysis

FoxO1	Mm00490672_m1	*Hey1*	Mm00468865_m1
FoxO3a	Mm01185722_m1	*Hey2*	Mm00468865_m1
FoxO4	Mm00840140_g1	*Jagged 1*	Mm00496902_m1
Flk1 (Kdr)	Mm00840140_g1	*Nrp1*	Mm00435379_m1
PECAM1	Mm01242584_m1	*Nrp2*	Mm00803099_m1
Tie2 (Tek)	Mm01242584_m1	*CoupTFII*	Mm00772789_m1
Flt1	Mm00438980_m1	*EphB4*	Mm01201157_m1
Connexin 43	Mm00438980_m1	*AFP*	Mm00431715_m1
eNOS	Mm00435217_m1	*ADM*	Mm00437438_g1
Connexin 37	Mm00433610_s1	*BMPER*	Mm01175806_m1
EphrinB2	Mm01215897_m1	*Sprouty2*	Mm00442344_m1
Notch1	Mm00435249_m1	*Sprouty4*	Mm00442345_m1
Dll4	Mm00444619_m1		